JYVÄSKYLÄ STUDIES IN COMPUTING
91

Timo Nihtilä

Performance of Advanced Transmission and Reception Algorithms for High Speed Downlink Packet Access

JYVÄSKYLÄN YLIOPISTO

JYVÄSKYLÄ STUDIES IN COMPUTING 91

Timo Nihtilä

Performance of Advanced Transmission and Reception Algorithms for High Speed Downlink Packet Access

Esitetään Jyväskylän yliopiston informaatioteknologian tiedekunnan suostumuksella
julkisesti tarkastettavaksi yliopiston Villa Ranan Blomstedt-salissa
huhtikuun 18. päivänä 2008 kello 12.

Academic dissertation to be publicly discussed, by permission of
the Faculty of Information Technology of the University of Jyväskylä,
in the Building Villa Rana, Blomstedt Hall, on April 18, 2008 at 12 o'clock noon.

UNIVERSITY OF JYVÄSKYLÄ

JYVÄSKYLÄ 2008

Performance of Advanced Transmission and Reception Algorithms for High Speed Downlink Packet Access

JYVÄSKYLÄ STUDIES IN COMPUTING 91

Timo Nihtilä

Performance of Advanced Transmission and Reception Algorithms for High Speed Downlink Packet Access

UNIVERSITY OF JYVÄSKYLÄ

JYVÄSKYLÄ 2008

Editors
Timo Männikkö
Department of Mathematical Information Technology, University of Jyväskylä
Irene Ylönen, Marja-Leena Tynkkynen
Publishing Unit, University Library of Jyväskylä

URN:ISBN:978-951-39-3249-7
ISBN 978-951-39-3249-7 (PDF)

ISBN 978-951-39-3236-7 (nid.)
ISSN 1456-5390

Jyväskylä University Printing House, Jyväskylä 2008

ABSTRACT

Nihtilä, Timo
Performance of Advanced Transmission and Reception Algorithms for High Speed Downlink Packet Access
Jyväskylä: University of Jyväskylä, 2008, 92 p.(+included articles)
(Jyväskylä Studies in Computing
ISSN 1456-5390; 91)
ISBN 978-951-39-3249-7 (PDF), 978-951-39-3236-7 (nid.)
Finnish summary
Diss.

This work studies the system level performance of several advanced techniques developed for Wideband Code Division Multiple Access (WCDMA) which is the most widely adopted technique for the air interface of 3rd generation (3G) wireless networks. The performance is evaluated particularly with High Speed Downlink Packet Access (HSDPA) concept of WCDMA. The analysis considers the performance of advanced signal reception algorithms in combination with antenna diversity techniques in various realistic HSDPA network scenarios. The performance of conventional Rake receiver is compared to a Linear Minimum Mean Squared Error (LMMSE) chip level equalizer being capable of intra- and inter-cell interference suppression. The receiver performance is evaluated with and without receive diversity and different transmit antenna diversity techniques, namely Space-Time Transmit Diversity (STTD) from open loop concepts and single and dual stream Transmit Antenna Array (TxAA) from the closed loop transmit diversity techniques. Also the impact of different HSDPA packet scheduling strategies, namely round robin and proportional fair scheduling, are observed. The performance evaluation is done by changing several network attributes such as UE velocity, channel profiles and cell sizes. The study is done by means of extensive system level simulations using a comprehensive dynamic WCDMA network simulation tool, which comprises detailed modeling of signal propagation models, user mobility, traffic models, physical layer, radio resource management (RRM) algorithms and part of the upper layers of a WCDMA radio access network.

Keywords: WCDMA, HSDPA, Rake, LMMSE, equalizer, receive diversity, transmit diversity, MIMO, TxAA, D-TxAA, STTD, system performance

Author
Timo Nihtilä
Department of Mathematical Information Technology
University of Jyväskylä
Finland

Supervisor
Professor Tapani Ristaniemi
Department of Mathematical Information Technology
University of Jyväskylä
Finland

Reviewers
Professor Zhisheng Niu
Department of Electronic Engineering
Tsinghua University
China

Dr., Docent Mikko Valkama
Institute of Communications Engineering
Tampere University of Technology
Finland

Opponent
Dr. Zekeriya Uykan
Nokia Siemens Networks
Finland

ACKNOWLEDGEMENTS

This thesis is done while working as a researcher in the Department of Mathematical Information Technology at the University of Jyväskylä from the beginning of 2004 to the beginning of 2006 and after that as a senior research scientist in Magister Solutions Ltd. The research was done in a co-operation project with Nokia. First of all, I want to thank all the parties involved in this project for allowing me the possibility to make this thesis and for the financial support during it.

Especially, I would like to thank my supervisor, Professor Tapani Ristaniemi, for taking me as a researcher to this project in the first place and for constant guidance during it and in the making of this thesis. I would like to thank my opponent Dr. Zekeriya Uykan and the reviewers of this thesis, Professor Zhisheng Niu and Dr., Docent Mikko Valkama. Special thanks to my colleague, Dr. Janne Kurjenniemi, for fruiful co-operation, invaluable advice and help during this project.

Thanks to Marko Lampinen, Elena Virtej and Ville Haikola from Nokia for co-authoring the included articles and also for supporting my simulation work in other ways. Also thanks to other people from Nokia: Jorma Kaikkonen and Sari Nielsen for supervising my research activities, Tero Henttonen and Mika Kolehmainen for providing help with the simulator and Jianke Fan and Markku Kuusela for support in some of the simulation campaigns. I would generally want to thank all the current and past colleagues in University of Jyväskylä, Magister Solutions Ltd and Nokia for being the most pleasant people to work with.

Thanks to Technological Foundation and Ulla Tuominen Foundation for financial support in the form of encouragement grants.

Big thanks to all my friends for their refreshing company, especially during the weekends. Clearing my mind regularly from work and research was very important to my mental wellbeing during the years. And what's a more efficient way of not thinking of soft handovers than suffering from hard hangovers...

Finally, I want to express my deepest gratitude to my parents Lasse and Pirkko, my brother Antti and especially to my girlfriend Jutta. Thank you all for being there for me and believing in me. I dedicate this thesis to you.

Jyväskylä, March 2008

Timo Nihtilä

Ah, there's nothing more exciting than science. You get all the fun of sitting still, being quiet, writing down numbers, paying attention... Science has it all.

Seymour Skinner

ACRONYMS

16QAM	16 Quadrature Amplitude Modulation
64QAM	64 Quadrature Amplitude Modulation
2G	2nd Generation mobile communication system
3G	3rd Generation mobile communication system
3GPP	3rd Generation Partnership Project
ACK	Acknowledgement
AMC	Adaptive Modulation and Coding
AOA	Angle of Arrival
AVI	Actual Value Interface
BER	Bit Error Rate
BTS	Base Transceiver Station
CC	Chase Combining
CDMA	Code Division Multiple Access
C/I	Carrier to Interference ratio
CIO	Cell Individual Offset
CL	Closed Loop
CL1	Closed Loop Mode 1
CLTD	Closed Loop Transmit Diversity
CN	Core Network
C-PICH	Common Pilot Channel
CSI	Channel State Information
CQI	Channel Quality Indicator
DL	Downlink
DCH	Dedicated Channel
DiffServ	Differentiated Services
DSCH	Downlink Shared Channel
D-TxAA	Dual stream Transmit Antenna Array
DTX	Discontinuous tranmission
ECR	Effective Coding Rate
EDGE	Enhanced Data rates for GSM Evolution
FACH	Forward Access Channel
FCS	Fast Cell Selection

FDD	Frequency Division Duplex
GHz	Gigahertz, 10^9 cycles per second
GPRS	General Packet Radio Service
GSM	Global System for Mobile communication
HARQ	Hybrid Automatic Repeat reQuest
HSDPA	High Speed Downlink Packet Access
HS-DPCCH	High Speed Dedicated Physical Control Channel
HS-DSCH	High Speed Downlink Shared Channel
HS-PDSCH	High Speed Physical Downlink Shared Channel
HS-SCCH	High Speed Shared Control Channel
Hz	Hertz, one cycle per second
I-LMMSE	Interference aware Linear Minimum Mean Squared Error
IR	Incremental Redundancy
ITU	International Telecommunication Union
ITU-R	ITU Radiocommunication sector
kB	Kilobyte
kbps	10^3 bits per second
kHz	Kilohertz, 10^3 cycles per second
LA	Link Adaptation
LMMSE	Linear Minimum Mean Squared Error
MAC	Medium Access Control
MAC-hs	Medium Access Control - High Speed
MAI	Multiple Access Interference
Mbps	10^6 bits per second
Mcps	10^6 chips per second
MCS	Modulation and Coding Scheme
MHz	Megahertz, 10^6 cycles per second
MIMO	Multiple Input Multiple Output
MMSE	Minimum Mean Squared Error
MRC	Maximum Ratio Combining
MUD	Multi-user detection
NACK	Negative Acknowledgement
PARC	Per-Antenna Rate Control
P-CPICH	Physical Common Pilot Channel

PDU	Protocol Data Unit
PedA	Pedestrian A
PF	Proportional Fair
PIC	Parallel Interference Cancellation
QoS	Quality of Service
QPSK	Quadrature Phase Shift Keying
RCQI	Relative CQI
RLC	Radio Link Control
RNC	Radio Network Controller
RNS	Radio Network Subsystem
RR	Round Robin
RRM	Radio Resource Management
RSCP	Received Signal Code Power
RSVP	Resource Reservation Protocol
Rx	Receiver
SF	Spreading Factor
SAW	Stop-And-Wait
SMS	Short Message Service
SNR	Signal to Noise Ratio
SINR	Signal to Interference and Noise Ratio
STTD	Space-Time Transmit Diversity
TDD	Time Division Duplex
TFRC	Transport Format and Resource Combination
TTI	Transmission Time Interval
Tx	Transmitter
TxAA	Transmit Antenna Array
UMTS	Universal Mobile Communication System
UE	User Entity
UL	Uplink
UMTS	Universal Mobile Telecommunication System
UTRAN	UMTS Terrestrial Radio Access Network
VehA	Vehicular A
WCDMA	Wideband Code Division Multiple Access
WLAN	Wireless Local Area Network
ZF	Zero-Forcing

LIST OF FIGURES

LIST OF TABLES

CONTENTS

LIST OF INCLUDED ARTICLES

PI T. Nihtilä, J. Kurjenniemi, M. Lampinen and T. Ristaniemi. WCDMA HSDPA Network Performance with Receive Diversity and LMMSE Chip Equalization. *Proceedings of the 16th International Symposium on Personal Indoor and Mobile Radio Communications (PIMRC'05), Berlin, Germany*, 2005.

PII J. Kurjenniemi, T. Nihtilä, M. Lampinen and T. Ristaniemi. Performance of WCDMA HSDPA Network with Different Advanced Receiver Penetrations. *Proceedings of the 8th International Symposium on Wireless Personal Multimedia Communications (WPMC'05), Aalborg, Denmark*, 2005.

PIII T. Nihtilä, J. Kurjenniemi, E. Virtej and T. Ristaniemi. Performance of Transmit Diversity Schemes with Advanced UE Receivers in HSDPA Network. *Proceedings of the 9th International Symposium on Wireless Personal Multimedia Communications (WPMC'06), San Diego, CA, USA*, 2006.

PIV J. Kurjenniemi, T. Nihtilä, E. Virtej and T. Ristaniemi. On the Effect of Reduced Interference Predictability to the HSDPA Network Performance with Closed Loop Transmit Diversity. *Proceedings of the 9th International Symposium on Wireless Personal Multimedia Communications (WPMC'06), San Diego, CA, USA, (***Best paper award***)*, 2006.

PV T. Nihtilä, J. Kurjenniemi, M. Lampinen and T. Ristaniemi. Performance of receive diversity and LMMSE chip equalization in WCDMA HSDPA network. *Wireless Personal Communications, No. 43, Vol. 2, pp. 261-280*, 2007.

PVI T. Nihtilä, J. Kurjenniemi and E. Virtej. System Level Analysis of Interference Aware LMMSE Chip Equalization in HSDPA Network. *Proceedings of the IEEE Symposium on Computers and Communications (ISCC'07), Aveiro, Portugal*, 2007.

PVII T. Nihtilä, J. Kurjenniemi and M. Lampinen. Effect of Ideal Inter-cell Interference Cancellation to HSDPA System Performance. *Proceedings of the 18th IEEE International Symposium on Personal, Indoor and Mobile Radio Communications (PIMRC'07), Athens, Greece*, 2007.

PVIII T. Nihtilä. Capacity Improvement by Employing Femto Cells in a Macro Cell HSDPA Network. *Proceedings of the 13th IEEE Symposium on Computers and Communications (ISCC'08), Marrakech, Morocco, (accepted for publication)*, 2008.

PIX T. Nihtilä. Increasing Femto Cell Throughput with HSDPA Using Higher Order Modulation. *2nd International Networking and Communications Conference (INCC'08), Lahore, Pakistan, (accepted for publication)*, 2008.

PX T. Nihtilä and V. Haikola. HSDPA MIMO System Performance in Macro Cell Network. *Proceedings of the 2008 IEEE Sarnoff Symposium, Princeton, NJ, USA, (accepted for publication)*, 2008.

The author of this thesis was the main author of article **PI** for which he participated in simulation scenario construction, conducted simulations and participated in the modelling and implementation work. In article **PII** the author participated in constructing the simulation scenarios, conducted the simulations and participated in writing of the article. The author of this thesis was the main author of article **PIII** and did part of the implementation and modelling work and conducted all the simulations. In addition to participating in the modelling and implementation work in article **PIV** the author contributed in simulation result analysis and in writing of the article. The author of this thesis was the main author in article **PV**, conducted most of the simulations and participated in the modelling and implementation of the studied schemes to the system simulator. The author was the main author in articles **PVI** and **PVII**, did all the modelling and conducted simulations and did the main part in result analysis. For articles **PVIII** and **PIX** the author was the single author, did all the modelling and simulation work and conducted the result analysis. The author was the main author in article **PX**, did all the modelling and conducted all the simulations and did the most part of the result analysis.

1 INTRODUCTION

Wireless communication industry gained huge success in the end of last millennium. In the 1980's the 1st generation mobile technology already enabled people to make voice calls independent on their location but the size and cost of the mobile handsets was a limiting factor in the popularity of 1st generation systems.

2nd generation (2G) telecommunication systems, such as the Global System for Mobile communications (GSM), started a real telecommunication avalanche introducing e.g. lower size and cost terminals and a new service, Short Messaging Service (SMS). The telecommunication field has grown ever since in all aspects. There has been a tremendous increase for example in the number of subscribers, mobile handsets, as well as operators and other wireless companies.

As this development was emerging, there was a clear need to enhance wireless communication beyond mere voice calls and SMS messages and to introduce new applications, transmission of multimedia as the most important one. However, many of the new applications required much higher data rate than what 2nd generation wireless networks were able to offer.

This lead to the design of 3rd generation (3G) systems that were able to offer higher bit rates than 2G systems. Wideband Code Division Multiple Access (WCDMA) is nowadays the most widely adopted air interface for 3G systems released in the Universal Mobile Telecommunication System (UMTS) frequency band at 2 GHz in Europe and Asia including Japan and Korea [Hol06]. WCDMA is specified by the 3rd Generation Partnership Project (3GPP) [3G07a], which is the joint standardization project of different 3G standardization bodies all over the world. The first 3G specification release of WCDMA was done in 1999, which is accordingly named Release '99. After this, four releases have been published, namely Releases 4, 5, 6 and 7, all of them enhancing the previous. Release 7 was closed in June 2007 and currently specification work concentrates on Release 8.

Applications are constantly evolving and increasing their data rate demands and the number of 3G subscribers increases. Thus the amount of data transmitted on the air keeps growing. In order to keep up with this development, continuous study is needed to enhance WCDMA performance. With many new applications, such as streaming video and other multimedia, more data is transmitted from the

base station to the mobile unit than vice versa. Due to this asymmetric data flow, particularly WCDMA downlink is expected to become the bottleneck of WCDMA system performance in the future.

Table 1 presents the comparison of peak data rates between different UMTS releases and 2G technologies, such as GSM, General Packet Radio Service (GPRS), Enhanced Data rates for GSM Evolution (EDGE). The maximum theoretical data rate supported by UMTS Release '99 is 2 Mbps for both uplink and downlink but it seems that the highest implemented data rate on the market is 384 kbps so far [Hol06]. In UMTS specification Release 5 High Speed Downlink Packet Access (HSDPA) was introduced to improve the capacity and spectral efficiency of the WCDMA downlink [Hol06, Kol03, Par01]. The theoretical peak data rate for Release 5 HSDPA is 14.4 Mbps. However, the actual user experienced peak data rates are much lower than this.

TABLE 1 Theoretical peak data rates of different telecommunication systems. [Rys06]

System	Peak data rate
GSM	14.4 kbps
GPRS	171.2 kbps
EDGE	473.6 kbps
Rel'99 WCDMA	2 Mbps
Rel 5 WCDMA (HSDPA)	14.4 Mbps
Rel 7 WCDMA (HSDPA+64QAM)	21.6 Mbps
Rel 7 WCDMA (HSDPA+MIMO)	28.8 Mbps

The latest 3GPP release included the support for higher order modulation 64 phase Quadrature Amplitude Modulation (64QAM) and the use of a dual stream Multiple Input - Multiple Output (MIMO) scheme with HSDPA. 64QAM increases the single stream peak data rates and using dual stream transmission the HSDPA theoretical peak data rate from Release 5 is doubled. So far 64QAM modulation is not supported with MIMO transmission mode but the support for that is expected to be in 3GPP Release 8.

Although Release 5 HSDPA already offers very good throughput to a mobile unit compared to 2G systems, there has been intense research to further improve the data rate of HSDPA in future specification releases. This thesis studies the technologies that have been adopted in releases 6 and 7 and their performance in comparison to each others. In the next chapter, the research problem of this thesis is addressed. Studies related to the problem are presented and discussed in chapter 1.2. In chapter 1.4 the outline of this thesis is presented.

1.1 Research problem

The studied technologies in this thesis can be divided into techniques that alter either the functionality of User Entity (UE) or the UMTS Terrestrial Radio Access Network (UTRAN) or both of them. Techniques that can be adopted altering only the UE side are advanced receiver structures and receive (Rx) antenna diversity. The features that can be adopted solely at the UTRAN side are advanced HSDPA packet scheduling, open loop transmit (Tx) diversity and the femto base station concept. Techniques that affect both UE and UTRAN side are closed loop transmit diversity techniques which require alterations both to the base station in the form of multiple transmit antennas and to the receiver where feedback calculation and the transmission of feedback information must be implemented.

1.1.1 Advanced reception algorithms

One of the main interference sources to a signal in WCDMA downlink are the multiple delayed replicas of the serving cell transmissions arriving at arbitrary time shifts at the UE receiver which compromise the orthogonality of downlink spreading codes. The interference is mainly present at frequency-selective channels and is called Multiple Access Interference (MAI). Advanced reception algorithms, such as using channel equalization at chip-level, are one option to mitigate the effect of MAI. In this thesis the main focus in the advanced receiver field is on one of the most prominent solutions the minimum mean squared error (MMSE) equalizer.

Although it is generally assumed that equalizer is used to cancel the interference caused by serving cell transmissions, it is also possible to use equalizer in order to suppress inter-cell interference as well. This so called interference aware equalizer is assumed to be aware of the neighboring sector channel situations and can estimate also their transmissions based on the temporal and more importantly the spatial characteristics of the interference using e.g. multiple antennas at the receiver. Thus, in this thesis it is studied what is the performance when also the inter-cell interference can be mitigated by equalization.

In this thesis a more general approach in advanced reception study is also taken by considering the effect of inter-cell interference mitigation in system performance point of view. Actual techniques are not considered but instead, the maximum achievable performance gains of different inter-cell interference mitigation efficiencies are charted in a fully loaded HSDPA network. The means or even the possibility to achieve the studied efficiencies are not considered. The system performance is evaluated with different receivers with and without receive diversity assuming some level of cancellation efficiency.

1.1.2 Receive diversity

Receive diversity is a powerful option when battling against signal fading at the UE side, especially at low power regions due to its power and diversity gain. The maximum performance can be achieved with uncorrelated receive antennas but since some distance between the antennas is required to achieve reasonable uncorrelation between them, this might be challenging considering the size of mobile units in general. Adopting multiple receive antennas increases both the cost and power consumption of the UE. These issues limit the applicability of receive diversity in reality. In this thesis the performance of receive diversity is evaluated with and without all the other studied techniques both at the UE and at the UTRAN side.

1.1.3 Transmit diversity

Transmit diversity has traditionally been considered a more feasible option than receive diversity. With open loop transmit diversity additional antennas and hardware modifications are adopted solely at the base station side. With closed loop techniques the added functionality at the receiver side is the feedback calculation, which is a relatively small modification. Thus the cost-effectiveness of transmit diversity schemes has been considered higher than receive diversity. However, although 3GPP specifications require transmit diversity support mandatory for the UE, practical implementations of transmit diversity have not been widely adopted so far.

Transmit and receive diversity provide equally good diversity gain but the technical aspects in the employment of transmit diversity are more complicated due to the loss of similar power gain as with receive diversity. This issue is more thoroughly addressed in chapter 4.2.

In this thesis the focus from the open loop transmit diversity techniques is in Space-Time Transmit Diversity (STTD) technique. Closed loop transmit diversity study is divided into two branches focusing on single and dual stream techniques. In both branches a technique called Transmit Antenna Array (TxAA) is considered. In single stream TxAA the transmitter uses two antennas to transmit a single transport stream as in dual stream TxAA (D-TxAA) two transport streams are transmitted simultaneously. The transmit antenna weights are selected in a way that the inter-stream interference is minimized. In good channel conditions D-TxAA can enhance HSDPA bit rate significantly. D-TxAA was selected as the MIMO technique for HSDPA in Release 7.

1.1.4 Advanced packet scheduling

The impact of different packet scheduling strategies are also studied. Using a simple round robin scheduling algorithm the scheduling time is allocated equally between users. However, using this kind of blind scheduling the inherent potential of the variating nature of the radio channel may be lost. Using an advanced

scheduling algorithm such as proportional fair in which users are scheduled in an opportunistic manner, the signal fading due to the radio channel can be turned into favour providing. Scheduling users at their best channel conditions introduces a new concept, multiuser diversity gain. Advanced packet scheduling offers the possibility to balance between user fairness and total system throughput. In this thesis the real potential of proportional fair is measured by comparing it to conventional round robin scheduling.

1.1.5 Femto base station concept

One potential solution to further increase the HSDPA bit rates is to introduce low transmission power base stations (BTS) in small isolated areas with insufficient or no macro cell coverage. These so called femto BTSs provide an access point mainly to home or small office users who benefit from high signal to interference ratios due to the proximity of the base station unit. Another advantage is that by using femto BTSs the network load is distributed to a higher number of access points, thus decreasing the waiting times and increasing the network performance in high load situations. Due to high serving cell signal level compared to neighboring cell signals in small cell sizes advanced receivers are expected to gain from the femto cell solution. The performance of different receiver schemes in femto cells is one of the results of this thesis.

1.1.6 Summary

The main questions this thesis answers are:

- What is the expected gain of an advanced UE reception algorithm, namely LMMSE chip level equalizer, over conventional rake reception on the system performance point of view?
- Do the observed gains vary when different realistic network situations are considered?
- How is the system performance affected when different penetration of advanced receiver UEs are gradually added to the network?
- What is the gain of inter-cell interference suppressing LMMSE equalizer over conventional LMMSE equalizer?
- What are the maximum achievable gains of inter-cell interference cancellation with different receivers?
- How does employing receive and/or different transmit antenna diversity techniques affect the observed gains with different receivers?
- Is there a difference in the achievable gains with advanced scheduling when different UE receivers and/or antenna diversity are used?

- How does employing small cells in the network affect the realized gains with different receivers?

To answer these questions, the performance of different receiver structures in combination with different antenna diversity schemes and scheduling strategies in various realistic situations in a WCDMA HSDPA network is studied by means of extensive dynamic system simulations, which are considered to reflect the real network behavior well. The network performance is analyzed first of all in terms of cell and user throughput. Cell throughput is the average instantaneous throughput of a cell and user throughput is defined as the average throughput experienced by a user during a call. Also signal quality and several other key performance indicators are used in the analysis.

1.2 Related studies and connection to thesis work

The performance of HSDPA network has been previously studied in e.g. [Kol02, Lov04, Ped04]. In [Kol02] the study considered different network setups and different packet scheduling strategies thus covering the tradeoff between user fairness and cell throughput. It was found that HSDPA performance is affected by multiple parameters, i.e. propagation environment, traffic characteristics and resource allocation policies.

In [Lov04] the system performance and physical layer aspects of HSDPA were considered using simulations. A comparison of HSDPA and Release '99 system was done with different traffic models. The main conclusion was that HSDPA offers 3 times better spectrum efficiency and cell and user throughput than a Release '99 system.

In [Tuo05] a spatial multiplexing approach to enhance the HSDPA system performance was introduced. Using receive and transmit diversity along with Per-Antenna Rate Control (PARC) a notable improvement in system performance compared to single stream diversity methods was observed in both flat-fading and frequency-selective fading channels. However, it was noticed that the improvement was mainly seen by users having high signal-to-interference ratios.

The MMSE chip-level equalizer receiver solution studied in this thesis was introduced in [Kra00a] and its bit error rate (BER) performance was compared to zero-forcing (ZF) equalizer and Rake receivers. It was found that MMSE equalizer BER performance is dramatically better than that of both ZF and Rake. These three receiver structures were later studied further in [Kra00b] where the BER performance comparison between antenna diversity and virtual channel diversity obtained through oversampling in a single received signal was presented. The obtained result was that spatial diversity is a more preferable solution than oversampling diversity. Furthermore, MMSE once again out-performed ZF and Rake receiver structures.

Linear intra-cell interference cancellation algorithms are previously studied also in [Hoo02] where the chip-level equalization in the WCDMA downlink

before despreading was discussed. LMMSE and zero-forcing equalizer solution were studied in link level. The results were compared to the performance of the Rake receiver. The results showed significant performance improvements of equalizer receivers over the conventional Rake receiver. On the other hand, parallel interference cancellation (PIC) algorithms that mitigate the intra-cell interference non-linearly was studied in [Div98].

There has also been a vast research in pursuit to suppress inter-cell interference efficiently. However, the studies have rarely considered the system level performance. In [Sch02] the authors evaluated the system performance of a non-linear iterative successive cancellation algorithm among Rake and LMMSE receivers. It was found that canceling inter-cell interference offers considerable system level gains both in indoor and vehicular channels.

A recent study of the WCDMA system performance for dedicated channels when a certain penetration of dual antenna terminals is assumed was presented in [Ram02]. This analysis was extended in [Ven03] where in addition to dual antennas chip equalizers are also considered. Clear capacity gains over conventional Rake-based dual antenna reception were observed if the dual antenna terminal penetration was high enough. In that study no code resource limitations were considered as in the simulations conducted in this thesis. In [Wan02] and [Lov03] the study was extended to the HSDPA network, where the Rake receiver and the LMMSE equalizer performance with and without receive diversity was analyzed. However, a quasi-static system level tool was used and hence no overhead on handovers was considered.

In [Oss04] transmit diversity techniques CL Mode 1, STTD and a system with two fixed beams were compared with system simulations. However, no receive diversity or advanced receivers were considered. Also in [Ram03] the system performance of receive diversity and CL Mode 1 and STTD transmit diversity schemes were studied with different packet scheduling strategies in HSDPA but no advanced receivers were considered.

System level performance of open loop transmit diversity techniques in combination with single and dual receive antennas in HSDPA were studied in [Maj04] but no advanced receivers or closed loop transmit diversity were covered. Performance analysis of the LMMSE equalizer in combination with multiple antenna schemes such as STTD and receive diversity was presented in [Pol04]. However, unlike the results presented in this thesis, the simulations were quasi-static and closed loop Tx diversity performance was not considered.

Recently in [Oss05] and [Rin05], system level studies for HSDPA with and without closed loop transmit diversity were presented. Based on those results the authors raised concerns that the reduced interference predictability results in an inherent problem for the CL Mode 1 to be used with HSDPA. Sudden interference fluctuations (termed a "flashlight" effect by the authors) together with the assumptions used in the studies resulted in the scheduler to function improperly. The results of [Oss05] and [Rin05] indicated that the usage of closed loop transmit diversity in HSDPA network is not advantageous at the cell boundaries.

On the other hand, another HSDPA study [Ber04] suggested that the HS-

DPA system is not impacted significantly by the increased interference variability due to TxAA thanks to the efficient hybrid automatic repeat request (HARQ) operation and inherent radio channel quality report errors of the system. This study did not include fully dynamic simulations, like the results presented in this thesis, but were based on pre-calculated interference effects from detailed link level studies.

Academic research has indicated MIMO transmission potential for high data rates [Fos98, Tel99, Ges03, Gol03] and several MIMO candidates were proposed for HSDPA in [3G07c]. The closed-loop MIMO schemes require knowledge of the channel impact in the transmitter, and hence in theory the closed-loop schemes have better performance than open-loop schemes. The D-TxAA benefits from channel knowledge, but still keeps the uplink feedback reasonable. Open-loop MIMO scheme was compared to receive diversity in [Lam05]. However, system performance evaluation of closed loop MIMO schemes for HSDPA have not been widely published. In [Hid06] D-TxAA was found to offer around 10 % gain in user throughput over receive diversity in an urban microcell spatial channel.

In this thesis, the above mentioned studies are extended in various fields. The receivers equipped with LMMSE chip-level equalizers with and without dual antenna receive and/or transmit antennas are evaluated in a full HSDPA network and present an analysis of the expected gains of different receiver - antenna diversity combination schemes over conventional single antenna Rake receiver in realistic situations by using a dynamic WCDMA system-level tool. From transmit diversity field an open loop concept called STTD is studied along with TxAA single stream closed loop transmit diversity technique. Also the performance of a closed loop MIMO technique D-TxAA is studied in a macro cell environment. The macro cell environment is a challenging scenario for MIMO transmission, because high signal to interference and noise ratios are experienced only near the base station. This leads to single stream usage of D-TxAA scheme in most cases and the gain of dual stream transmission is not achieved.

Both the code resource limitation and the most essential radio resource management algorithms are modeled in detail. The impact of different packet scheduling strategies is considered. The study also covers different UE velocities to some extent and channel power delay profiles in order to evaluate the robustness of advanced receivers in different channel conditions.

Moreover, it is reasonable to assume that not all the receivers are advanced ones immediately but the penetration of them in the network is an increasing factor. Therefore the dynamic behavior of the system needs to be analyzed from the network and end-user perspective, i.e. how much gain is seen in the cell throughput when advanced receiver penetration is increased and how the fairness of different users is maintained in terms of user throughput. The WCDMA HSDPA network performance is thus evaluated also from this point of view by assuming that the penetration of a certain advanced receiver type is gradually increased in the network.

In this thesis it is also studied whether the claimed "flashlight" effect is present in HSDPA network with closed loop transmit diversity. The study is done

by means of dynamic system level simulations. Moreover, in the performed simulations the effect of intra-cell and inter-cell interference is explicitly modeled. This is in contrast to the modeling in [Rin05] where the interference was based on orthogonality matrix approximation.

1.3 Other articles

In addition to the included articles, the author of this thesis has also published several other articles considering 3G system quality of service (QoS) which are not included in this thesis.

1. E. Wallenius, T. Hämäläinen, T. Nihtilä, J. Puttonen, J. Joutsensalo, Simulation Study on 3G and WLAN Interworking, *IEICE Transactions on Communications, Vol. E89-B, No. 2, pp. 446-459*, 2006.

2. E. Wallenius, T. Hämäläinen, T. Nihtilä, K. Luostarinen, J. Joutsensalo, 3G/4G interworking with WLAN QoS 802.11e, *Proceedings of the IEEE Semiannual Vehicular Technology Conference, (VTC Fall 2003)*, October 2003, Orlando, USA.

3. T. Hämäläinen, E. Wallenius, T. Nihtilä, K. Luostarinen, End-to-End QoS Issues at the Integrated WLAN and 3G Environments, *Proceedings of the 9th Asia-Pacific Conference in Communications (APCC 2003)*, September 2003, Penang, Malaysia.

4. T. Hämäläinen, E. Wallenius, T. Nihtilä, K. Luostarinen, Providing QoS at the Integrated WLAN and 3G Environments, *Proceedings of the 14th IEEE International Symposium on Personal, Indoor and Mobile Radio Communications (PIMRC 2003)*, October 2003, Beijing, China.

5. E. Wallenius, T. Hämäläinen, T. Nihtilä, J. Joutsensalo, 3G and WLAN Interworking QoS Solution, *Proceedings of the 5th IEEE International Conference on Mobile and Wireless Communications Networks (MWCN 2003)*, September/October 2003, Singapore.

6. E. Wallenius, T. Hämäläinen, T. Nihtilä, J. Joutsensalo, Providing QoS in 3G-WLAN Environment with RSVP and DiffServ, *Proceedings of the 1st International Conference on E-business and Telecommunication Networks (ICETE 2004)*, August 2004, Setúbal, Portugal.

1.4 Outline

In chapter 2 an introduction to UMTS and WCDMA technology is presented first. Then HSDPA concept and its features are discussed in more detail. In chapter 3 different UE receiver structures are presented and the mathematical modeling

of them and the general WCDMA signal model are presented. In chapter 4 the basics of receive and transmit antenna diversity are presented. Also different techniques used in WCDMA and their modeling is presented and discussed in detail. In chapter 5 the research tool is introduced and the achieved results are presented. Finally, in chapter 6 conclusions are drawn.

2 HIGH SPEED DOWNLINK PACKET ACCESS IN WCDMA

The HSDPA concept has been widely covered in [Hol06, Kol03, Par01] and the physical layer aspects of it can be found in 3GPP specifications [3G01]. In this chapter a brief introduction to HSDPA is presented. First, the general structure and features of UMTS and its air interface WCDMA is covered in chapters 2.1 and 2.2, respectively. In chapter 2.3 the enhancements of HSDPA technology to WCDMA downlink is presented.

2.1 UMTS architecture

The architecture of the UMTS system is depicted in Fig. 1. It consists of such logical network elements as core network (CN), user equipment (UE) and UMTS Terrestrial Radio Access Network (UTRAN) [3G04b]. The core network is responsible for routing connections between external networks and UMTS. It is connected to UTRAN via Iu interface. UTRAN handles all radio related functionality in UMTS.

UTRAN includes one or more Radio Network Subsystems (RNS), which consists of one Radio Network Controller (RNC) and at least one Node B (or base station) [3G06b]. RNC owns and controls all Node Bs in its domain. RNCs are connected to each other through the Iur interface and Node Bs to RNC via Iub interace. UTRAN is ultimately connected to the UEs via the Uu interface, which is the WCDMA air interface.

2.2 Basics of WCDMA

WCDMA physical layer has unique features that make it different from other multiple access schemes. In this chapter the main characteristics of basic WCDMA

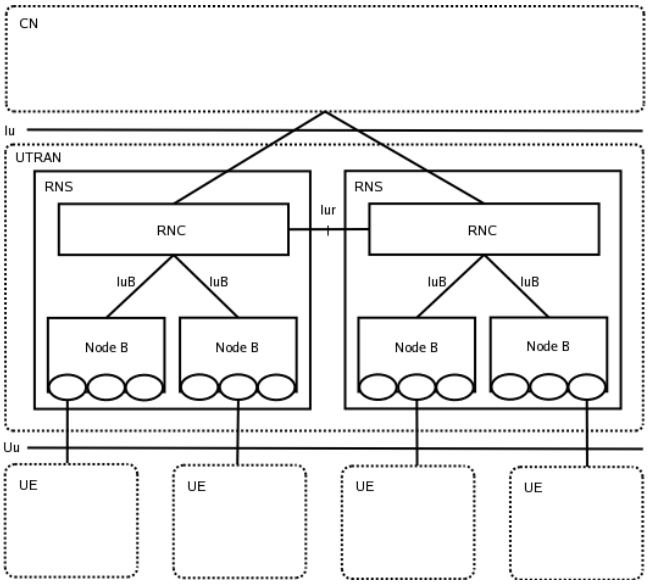

FIGURE 1 UMTS architecture [3G04b, 3G06b].

operation specified in Release '99 and Release 4 is discussed more thoroughly.

2.2.1 Code Division Multiple Access technology

In WCDMA user data bits are spread over a wide bandwidth by multiplying them by pseudorandom spreading sequences consisting of very short duration bits called chips. Different users data is spread with different chip sequences (spreading codes) which have low cross-correlation values to each other. In the downlink they are entirely orthogonal. As each user is operating on the same frequency, their signals get mixed up at the receiver. Due to the low correlation of the spreading codes each user data can be recovered from the received signal by multiplying it with the same code used in spreading, hence the term Code Division Multiple Access. The length of the spreading code per data bit is called the spreading factor (SF). Channels maximum physical layer bit rate per code channel is inversely proportional to the spreading factor.

The chip rate determines the operating bandwidth of the WCDMA system. 3.84MHz chip-rate maps into approximately 5 MHz bandwidth. The wide bandwidth offers several benefits such as support for high data rates and increased multipath diversity.

2.2.2 Power control

Spreading codes are used to separate different users in the uplink and different channels in the downlink. As different transmissions use the same bandwidth,

the signals interfere with each other. To minimize the interference in WCDMA system the signal powers need to be controlled. The objective is to transmit with minimal power that is needed to receive the signal with acceptable quality. As channel variations cause the signal to fade very rapidly, the power control needs to be fast in order to maintain a constant received power level at the receiver. In WCDMA transmitter power is controlled by the inner loop power control at the rate of 1500 Hz.

The inner loop power control is based on a closed loop algorithm. The receiver measures the signal to noise ratio (SNR) of the received signal and compares that to the target. If the signal is below the target, the receiver tells the transmitter to increase its power and vice versa. Outer loop power control is then responsible for measuring the signal quality and altering the signal level target to which the received signal is compared. Outer loop power control is adjusted in 10 ms intervals (after each received radio frame). If a frame is received correctly, the SNR target is decreased. If an error occurs, target is increased.

2.2.3 Soft handover

As all Node Bs in WCDMA system are transmitting with the same frequency, this allows a user to be connected to more than one Node B at a time. This connection type is generally called soft handover. If a user measures that the power levels of more than one sector belonging to the same or a different Node B are adequately good, the user can establish a soft handover connection to them. The connection to two or more sectors of the same Node B is called softer handover. If the connection is between multiple sectors belonging to different Node Bs, it is called a soft handover.

Soft/softer handover decreases both the uplink and downlink interference levels. In the uplink the signal sent by the UE is received by multiple sectors. Their received signals can be combined and thus the UE does not need to transmit with as high power as if it would be connected only to a single sector. The same effect takes place in the downlink. The sectors can transmit with lower power as the UE can combine the received signals.

On the other hand, the code resources for one user need to be reserved from multiple sectors and thus excessive soft handover connections can limit the capacity.

2.2.4 Release '99 WCDMA downlink

Downlink packet data transmission is already supported in Release '99. The channel possibilities to use a packet data service in the specifications are

- Dedicated Channel (DCH),
- Downlink Shared Channel (DSCH) and
- Forward Access Channel (FACH).

DCH has a fixed spreading factor in the downlink i.e. it reserves the code capacity according to the maximum bit rate of the connection. This is not the most efficient use of code resources since a lot of applications' bit rate demands vary significantly during the connection. With these applications a big portion of code resources would be wasted during low activity periods.

DSCH always operates alongside DCH and it is meant mainly for packet data. It's has a dynamically varying SF in 10 ms periods. Its code resources can be divided between users and it supports single code or multicode transmission. DSCH can be fast power controlled with the associated DCH but it does not support soft handover.

FACH is operated normally on its own with a fixed spreading factor and a rather high power to reach all users in the cell. FACH does not support fast power control or soft handover [Hol06].

2.3 High Speed Downlink Packet Access

This chapter presents the basic architecture and features of WCDMA HSDPA concept [Hol06, 3G06c]. HSDPA was introduced in 3GPP Release 5. The purpose was to increase Release '99 and Release 4 downlink packet data transmission performance. Three new channels were introduced with HSDPA [3G05]. All the user data is carried on the high speed downlink shared channel (HS-DSCH). Its associated control channel is the high speed shared control channel (HS-SCCH). Uplink control channel is the high speed dedicated physical control channel (HS-DPCCH). The channels are more thoroughly addressed in chapter 2.3.6.

As Release '99 packet data transmission using DCH, DSCH and FACH channels can be considered as quite static and slow in nature, HSDPA offers a fast and dynamic transmission scheme efficiently utilizing the potential inherent in WCDMA technology. This is achieved through several advanced techniques presented in the following chapters.

2.3.1 Link adaptation

Basic WCDMA functionality in Release '99 follows the changes in link quality with fast power control and targets to keep the received downlink SNR equal between different users. In HSDPA the spreading factor and the link power (if static power allocation is used) of the user data channel are kept constant but the quality of the link is tracked by the UE and reported to the Node B by the *link adaptation (LA)* function in order to exploit and to adapt to the dynamic variations in link quality.

Each UE sends a periodic channel quality indicator (CQI) message at each transmission time interval (TTI) to the Node B. The CQI indicates the maximum transport block the UE can receive with not more than 10 % error probability at the current channel situation. UE measures the Common Pilot Channel (C-PICH)

signal strength and sends an integer between 0 and 30 which corresponds to the pilot carrier to interference ratio (C/I). Node B first compensates the CQI with the power offset between the C-PICH and HS-DSCH. In Node B there is also a link adaptation outer loop operational, which corrects the received CQI with a specific correction factor [Ped04, Nak02]. The correction factor is altered based on the success of past transmissions. If the error probability of sent transport blocks is higher than the target, reported CQI is lowered to ensure a more reliable transmission and vice versa.

2.3.2 Adaptive modulation and coding

HSDPA packet data transmission is based on the idea that link quality dictates the amount of transmitted data. The user downlink bit rate is adjusted by *adaptive modulation and coding (AMC)* and effective multicode operation according to the CQI feedback from the UE.

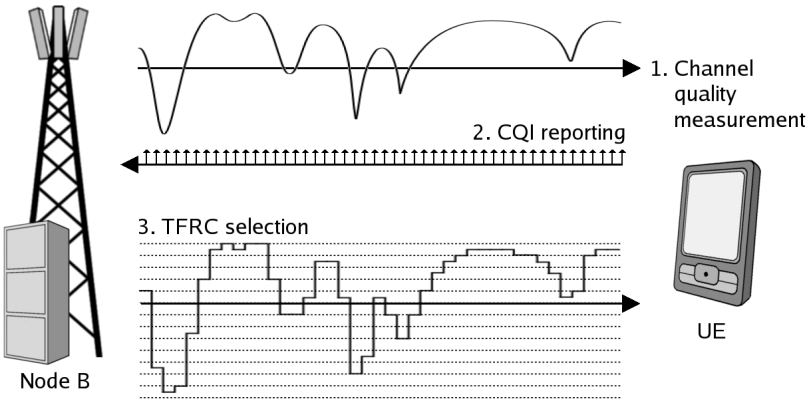

FIGURE 2 Adaptive modulation and coding.

Modulation and coding scheme (MCS) or transport format and resource combination (TFRC) of the next transmission to the UE is selected in Node B according to the compensated and corrected CQI report sent by the UE, as depicted in Fig. 2. In good link conditions a higher MCS is selected, which can transmit more bits but is more prone to errors. In poor channel conditions a more robust MCS is used with the cost of throughput. Although AMC is a more complicated functionality than fast power control, it offers power efficiency gain due to the elimination of power control overhead [Kol03]. The means of adaptation are transport block size, modulation scheme, effective coding rate (ECR), number of used multicodes, and transmission power per code.

With a higher amount of multicodes a higher number of adjacent downlink code channels can be used to transmit the information, thus achieving higher throughput. The theoretical maximum number of available multicodes is equal to the spreading code length, which is 16 with HS-DSCH but one code is reserved

for common channels and the associated DCH. Thus, up to 15 multicodes can be allocated for HSDPA user data transmission.

Two different modulation techniques are used in Release 5 HSDPA: quadrature phase shift keying (QPSK) which is used also with DCH and a higher order 16 phase quadrature amplitude modulation (16QAM). QPSK is more robust enduring lower channel quality whereas 16QAM offers higher throughput but requires a higher signal to interference and noise ratio (SINR) for good performance.

However, in indoor situations the SINR can be so high that even with 16QAM, highest ECR (lowest coding protection) and with highest amount of used multicodes the bit error probability is still lower than the target. This means that more bits could be delivered with acceptable quality. Therefore, the superior signal quality is not fully exploited and resources are wasted. In exceptionally good link conditions 64QAM is an option to achieve larger transport block sizes than with 16QAM or QPSK. 3GPP Release 7 included the possibility to use 64QAM with HS-DSCH [3G07b]. The constellation diagrams of QPSK, 16QAM and 64QAM are presented in Figure 3. 64QAM delivers most bits per symbol but the smallest distance between adjacent symbols makes 64QAM also most susceptible to symbol errors of the presented modulation schemes.

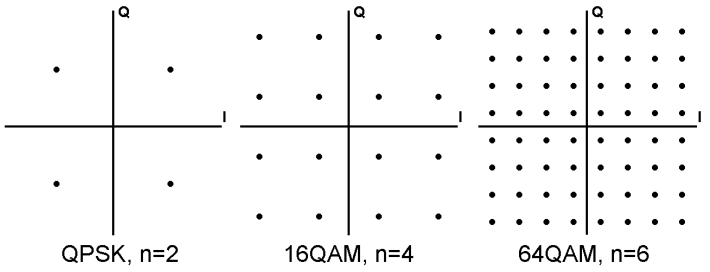

FIGURE 3 Modulation constellation diagrams and transmitted bits per symbol (n).

Another link adaptation technique is to change the coding rate of the transmission according to the link quality. This means that the transmitted bit stream is added with coding bits so that despite possible bit errors due to poor channel quality the original payload bits can still be retrieved from the received bit stream. Higher coding protection results in a more error robust transmission but naturally fewer number of payload bits can be delivered, which decreases the achievable throughput.

If in exceptionally good channel conditions the error probability target is not reached by using other adaptation techniques (modulation, number of multicodes, ECR) it is also possible to use lower the transmission power per code. This does not increase the achieved bit rate but it decreases the interference caused to other users.

The link adaptation dynamics for each UE depends on the UE capability to

support the different adaptation techniques. Especially in the early phase of HSDPA deployment, all devices will not necessarily support, for example 16QAM modulation or more than five parallel codes.

Table 2 presents the UE categories decided for 3GPP Release 7 and the maximum number of supported multicodes, supported modulations and their maximum ECR. Categories 9M and 10M terminals support MIMO mode operation i.e. dual stream transmission where two transport blocks are transmitted simultaneously using the same multicodes. Thus, the 9M and 10M category MCSs each have the same number of multicodes and the transport blocks for both streams are allocated from the same table according to their individual CQI reports. MIMO operation is more thoroughly addressed in chapter 4.2.4.

In Table 3 an example of an MCS table for UE categories 7 and 8 is presented. Category 7 and 8 UEs support a maximum of 10 multicodes used for HSDPA. QPSK and 16QAM modulations are supported. As the link adaptation dynamics are limited by the number of multicodes, in the high end of the MCS table the reference power offset is taken into use with these UE categories. Reference power offset represents the power decrease per code compared to normal power allocation per code.

TABLE 2 Terminal categories in HSDPA.

Terminal category	Maximum no. of multicodes	Modulations supported	Maximum ECR
1-6	5	QPSK	0.69
		16QAM	0.75
7-8	10	QPSK	0.69
		16QAM	0.75
9	12	QPSK	0.69
		16QAM	0.75
10	15	QPSK	0.69
		16QAM	0.89
11-12	5	QPSK	0.69
13	14	QPSK	0.69
		16QAM	0.75
		64QAM	0.80
14	15	QPSK	0.69
		16QAM	0.75
		64QAM	0.89
9M (*	15	QPSK	0.69
		16QAM	0.77
10M (*	15	QPSK	0.69
		16QAM	0.92

*) For terminals supporting MIMO operation

HS-DSCH physical layer transport block size per TTI (2 ms) can be derived straight from the chip rate, spreading factor (SF=16 for HS-DSCH), modulation (bits per symbol), effective coding rate and number of multicodes, as shown in Eq. 1.

$$\begin{aligned} blockSize[bits] &= \frac{chipRate}{SF*TTIsPerSecond} * bitsPerSymbol * ECR * noOfCodes \\ &= 480 * bitsPerSymbol * ECR * noOfCodes\,. \end{aligned} \tag{1}$$

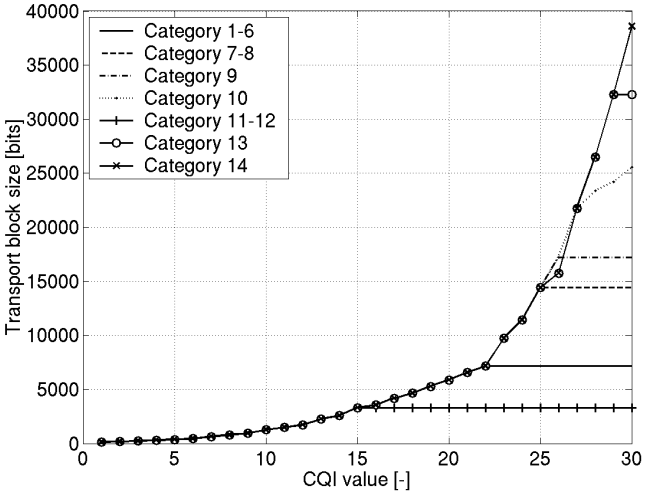

FIGURE 4 Allocated transport block size in relation to CQI value.

In Fig. 4 the relationship between the allocated transport block size and the reported CQI value, which represents the signal quality, is presented for different UE categories. It can be seen that the higher number of codes reserved for HSDPA offers increasingly high throughput with better signal quality. With high SINR values the performance of HSDPA can be severely limited by the code resources.

2.3.3 Fast physical layer retransmissions

Also the retransmission functionality has been improved in HSDPA. In Release '99 the retransmissions of an incorrectly received packet are RNC controlled. This causes signaling between the RNC and the Node B and results in long delays in packet transmission. In HSDPA, an additional Medium Access Control (MAC) entity, MAC-hs, has been added to Node B which is responsible for another advanced feature of HSDPA, *fast physical layer retransmissions*. Employing Node B controlled retransmissions results in less delay jitter than with RNC controlled retransmission scheme and it is very attractive for data services such as Transmission Control Protocol (TCP). The retransmission functionality is depicted in

TABLE 3 An example MCS table for category 7 and 8 UEs.

CQI value	Transport block size [bits]	No. of multicodes	Coding rate	Modulation	Reference power offset [dB]
1	137	1	0.14	QPSK	0
2	173	1	0.18	QPSK	0
3	233	1	0.24	QPSK	0
4	317	1	0.33	QPSK	0
5	377	1	0.39	QPSK	0
6	461	1	0.48	QPSK	0
7	650	2	0.34	QPSK	0
8	792	2	0.41	QPSK	0
9	931	2	0.48	QPSK	0
10	1262	3	0.44	QPSK	0
11	1483	3	0.51	QPSK	0
12	1742	3	0.60	QPSK	0
13	2279	4	0.59	QPSK	0
14	2583	4	0.67	QPSK	0
15	3319	5	0.69	QPSK	0
16	3565	5	0.37	16QAM	0
17	4189	5	0.44	16QAM	0
18	4664	5	0.49	16QAM	0
19	5287	5	0.55	16QAM	0
20	5887	5	0.61	16QAM	0
21	6554	5	0.68	16QAM	0
22	7168	5	0.75	16QAM	0
23	9719	7	0.72	16QAM	0
24	11418	8	0.74	16QAM	0
25	14411	10	0.75	16QAM	0
26	14411	10	0.75	16QAM	-1
27	14411	10	0.75	16QAM	-2
28	14411	10	0.75	16QAM	-3
29	14411	10	0.75	16QAM	-4
30	14411	10	0.75	16QAM	-5

Fig. 5. In the figure there is illustrated an example of the transmission strategy of a Radio Link Control (RLC) Protocol Data Unit (PDU). The PDU is sent by RNC to Node B to the UE specific PDU buffer. Node B constructs a HSDPA transport block from RLC PDUs in the buffer and sends it to the UE.

When the transport block is successfully received, the UE sends an acknowledgement (ACK) of the transport block to the Node B, which forwards the RLC ACKs to RNC. If the transport block is not successfully received after the maximum number of retransmissions, an RLC negative acknowledgement (NACK) is sent, which triggers the RLC retransmission of lost packet(s), if the RLC acknowledgement mode is used. However, RLC retransmissions are usually needed only in HSDPA sector handovers, which are hard handovers and some packet loss might occur. Since the physical layer retransmissions are handled in Node B, the ACK/NACK signaling can be executed between UE and Node B with very minimal delay.

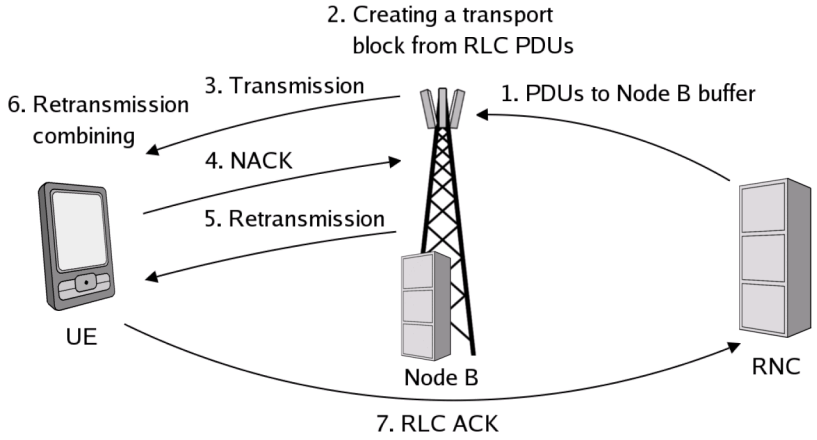

FIGURE 5 Retransmission functionality in HSDPA.

Due to the long delays in Release '99 retransmission functionality the information of previous transmissions cannot be utilized at all when detecting retransmissions, making all transmission attempts totally independent. Due to the small retransmission delay of HSDPA the utilization of the previous transmissions is enabled. Using the *hybrid automatic repeat request (HARQ)* functionality the energy of different transmission attempts of a transport block can be combined and thus be able to increase the probability to receive the transmission correctly. Buffering the previous transmissions however requires memory from the UE. The retransmission can be either identical to the first transmission which is called chase combining (CC) [Cha85] or contain different bits compared with channel encoder output that was received during the last transmission that is referred as incremental redundancy (IR). With IR one can achieve a diversity gain as well as improved decoding efficiency. Performance and modeling of CC and IR for system simulations are presented in [Fre02].

2.3.4 Fast scheduling at Node B

HSDPA scheduling is quite different from the DCH scheduling. DCH reserves code resources for the whole TTI according to the peak data rate of the connection during the TTI. If the TTI period is long, the application may lower its data rate demands during that and code resources are wasted.

To increase the efficiency of the resource allocation HSDPA transmission is divided into short TTIs of 3 time slots (2 ms). The use of short TTI length enables the dynamic resource sharing between users by the *fast scheduling at Node B*. With HSDPA all usable data transmission resources are used for a single user at each TTI separately. If a user has no data to transmit in a TTI, the resources of that TTI are allocated to some other user with data to transmit.

2.3.5 Packet scheduler

The basic purpose of the packet scheduler is to share the HS-DSCH resources between users eligible for receiving data. The scheduling decision of a user is done in HSDPA by the packet scheduler and can be based on several issues:

- quality feedback from the UE,
- UE data reception capability,
- resource availability,
- data buffer status and
- quality of service (QoS) and priority of data.

The scheduling algorithm can be based on all or some of the listed items. However, the two main parameters of the scheduler is the importance of

1. maintaining efficient HS-DSCH utilization and
2. sharing resources fairly between users.

Either point would be easy to fulfill if the other part would not have to be taken into account. Discarding the first clause, always scheduling the user with the best signal quality maximizes the network throughput. Maximum carrier to interference ratio (Max C/I) or maximum throughput scheduler is an implementation of this. It allocates HS-DSCH resources solely to users with a high channel quality. With this scheduler the worst signal quality users may never be scheduled.

On the other hand, highest order fairness is realized when every user is scheduled equally no matter what their signal quality is at the moment of scheduling. Round robin is this kind of scheduler in HSDPA.

In order to offer the best possible quality of service to all users while maintaining efficient HS-DSCH utilization is a challenging task. One solution to this task is to exploit the nature of multipath fading channels. When fading occurs

the signal power variates from very low to very high. As users' signals fade independently it is always beneficial to allocate channel resources to the user whose channel is at its peak. With this kind of scheduler the HSDPA system is able to benefit from the short term variations of the channel and to utilize the multiuser diversity gain inherent in fading channels.

Proportional fair scheduler

One scheduling algorithm which takes into account both the expected throughput and the fairness of resource sharing is the proportional fair (PF) scheduler [Hol00]. PF calculates a relative CQI (RCQI) for each user using the expected throughput (signal quality) and the amount of previously transmitted data (fairness) as parameters. The user which has the highest relative CQI is scheduled. The relative CQI for user k at scheduling interval (TTI) n can be defined as

$$\mathrm{RCQI}_k[n] = \frac{R_k[n]}{T_k[n]} = \frac{\min\left\{\mathrm{CQI}_k[n], \frac{B_k}{t_{TTI}}\right\}}{T_k[n]}, \tag{2}$$

where $R_k[n]$ is the user k's supported throughput in the next TTI, $T_k[n]$ is the average delivered user throughput in the past, $B_k[n]$ is the amount of data pending for user k at the current TTI, and t_{TTI} is the TTI length, 2 ms. The amount of data in the buffer for the user is taken into account in order to reduce the possibility of wasted channel capacity due to the scheduling of a user with a low amount of data in good channel conditions. The "min" function is disabled after 1 second to avoid excess delays when buffer occupancy is low. The average delivered throughput is calculated recursively as

$$T_k[n] = \left(1 - \{B_k[n] > 0\} \cdot \frac{1}{N_k}\right) T_k[n-1] + \frac{1}{N_k} R'_k[n-1], \tag{3}$$

where N_k is the forgetting factor, R'_k is the actual throughput transmitted to the UE at the nth TTI. The $\{B_k[n] > 0\}$ term is either 1 or 0 depending on whether there is data in the Node B buffer for user k or not.

The forgetting factor is an important parameter in proportional fair scheduling. It defines how much weight is given for signal quality and how much for the fairness. With the forgetting factor, it can be decided whether PF scheduling behavior resembles more Max C/I or round robin scheduling.

The basic idea of the scheduling algorithm is presented in Fig. 6. In the figure UE 1 is scheduled first. As the expected throughput (signal strength) of UE 2 increases, it gets the scheduling turn at time t_1 although UE 1 has a higher expected throughput. This is due to UE 2 having low average delivered throughput which increases its priority metric over UE 1, which has high average delivered throughput. As UE 2 signal strength decreases UE 3 gets the scheduling turn at time t_2 for the same reason over UEs 1 and 2. All the time UE 1 is not scheduled, its average delivered throughput decreases. After UE 3 signal worsens, UE 1 gets the scheduling turn back at time t_3 due to its good signal quality in addition to low average delivered throughput in the past.

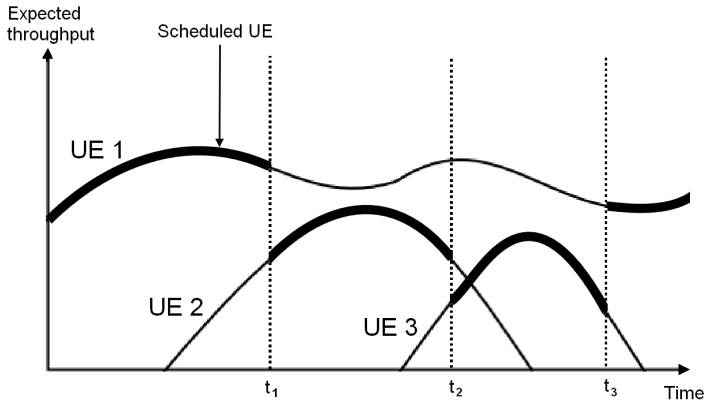

FIGURE 6 Proportional fair scheduling.

2.3.6 Channels in HSDPA

In this chapter the HSDPA user data channel HS-DSCH, its associated signaling channel HS-SCCH and the uplink control channel HS-DPCCH are discussed.

High speed downlink shared channel

HS-DSCH is the user data channel in HSDPA. It is mapped to the high speed physical downlink shared channel (HS-PDSCH) in the physical layer. The differences between main user data channel in Release '99, DCH and HS-DSCH have been listed in Table 4.

TABLE 4 Differences between DCH and HS-DSCH.

Feature	DCH	HS-DSCH
Spreading factor	Variable, 4-512	Fixed, 16
Fast power control	Yes	No
Soft handover support	Yes	No
Multi-code operation	Yes	Yes, extended
Adaptive modulation and coding	No	Yes
Physical layer retransmissions	No	Yes
Node B based scheduling	No	Yes
Link adaptation	No	Yes
TTI length	10, 20, 40 or 80 ms	2 ms
Modulation	QPSK	QPSK/16QAM/ 64QAM

High speed shared control channel

HS-SCCH is the associated signaling channel in HSDPA. The timing between HS-SCCH and HS-DSCH is done so that HS-SCCH begins its transmission two time slots before HS-DSCH to inform the UEs which of them is scheduled and to transport demodulation information to the scheduled UE. The timing between HS-DSCH and HS-SCCH is depicted in Fig. 7. Normally there is just one HS-SCCH transmitted in a TTI but if more than one user is scheduled (i.e. code multiplexing is used), a separate HS-SCCH has to be transmitted to all scheduled users. HS-SCCH transmit power can be static or it can be power controlled. HS-SCCH has a fixed spreading code of 128, which means that during one TTI (3 slots) it is able to transmit 40 bits of data with QPSK modulation.

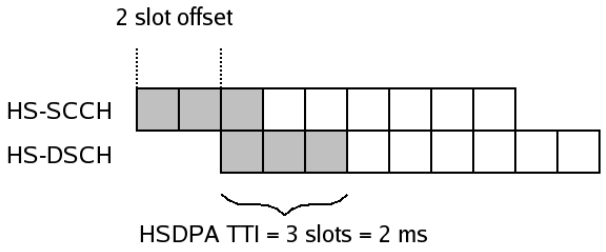

FIGURE 7 HS-SCCH and HS-DSCH timing.

HS-SCCH power control is needed to minimize the HS-DSCH interference whilst maintaining adequate HS-SCCH signal quality. The 3GPP specifications do not specify any power control mechanism for HS-SCCH. However, HS-SCCH power control can be based on

- HS-DPCCH power control commands or
- CQI reports.

As associated DPCCH is power controlled by the UE, its information can be used in setting the HS-SCCH power with an offset. Also the CQI reports are a good indicator of the channel between Node B and the UE.

High speed dedicated physical channel

The high speed dedicated physical control channel is used for uplink signalling in HSDPA. HS-DPCCH transmits CQI messages used in link adaptation functionality. Also packet acknowledgements (ACK) and negative acknowledgements (NACK) are transmitted in this channel to be utilized in the HARQ operation.

2.3.7 Radio resource management in RNC

Radio resource management (RRM) algorithms are needed to utilize the physical layer improvements of HSDPA to ultimately benefit end users. RRM functionality is divided between the RNC and Node B. At RNC, new HSDPA related RRM algorithms are resource allocation, admission control and mobility management.

Resource allocation

Resource allocation is responsible for allocating power and channelization codes to Node B for HSDPA in each cell. It is generally more advantageous to allocate as many channelization codes for high speed physical downlink shared channel (HS-PDSCH) as possible since the spectral efficiency of HS-DSCH is therefore improved. Allocating more codes for HSDPA usage leaves less codes for other channels. This might eventually result in call blocking of Release '99 users. However, RNC may release HS-PDSCH codes rapidly in case of code congestion.

If HSDPA mobiles support fewer codes than what is available in Node B, code multiplexing can be employed. After allocating resources to one UE, Node B can allocate left over resources to other users, increasing the resource utilization efficiency. Fig. 8 presents an example of scheduling and code resource allocation when code multiplexing is enabled. After scheduling of the primary user the rest or a portion of the leftover multicodes are allocated to another user. After the scheduling of the secondary user there still might be unallocated code space left if there is more codes left than what the users CQI report suggests to be used and there is no users. On the other hand, the number of scheduled users per TTI is limited only by the number of codes.

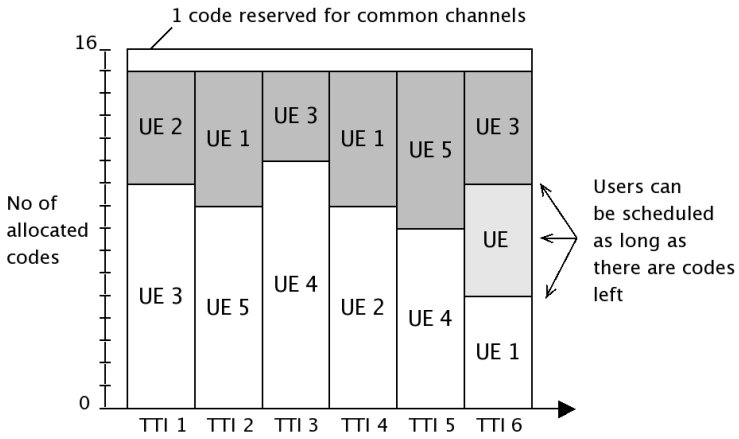

FIGURE 8 Example of code allocation with code multiplexing.

However, in most cases the most limited downlink transmission resource is power. Power has to be allocated for common channels, such as physical com-

mon pilot channel (P-CPICH) and DCH and also to HSDPA channels HS-SCCH and HS-DSCH. Two options exist in power resource allocation between HSDPA and common channels. The first option is to use static power allocation for HSDPA. Node B reserves some amount of power for HSDPA, which is distributed between HS-DSCH and HS-SCCH. Common channels use the rest of the power and cannot use HSDPA power even temporarily although HSDPA would be inactive. RNC can update the static power allocation for HSDPA at any time. The second option is to use dynamic power allocation in which Node B first allocates power to common channels (C-PICH, associated DCH) and then allocates all unused power for HSDPA. Fig. 9 presents an example of both static and dynamic power allocation modes. With dynamic power allocation the maximum Node B transmission power can be achieved without the need for clipping common channel powers.

Ultimately RNC is responsible for the quality of both DCH and HSDPA calls. The power distribution between these two can therefore be done according to call QoS parameters of both channels.

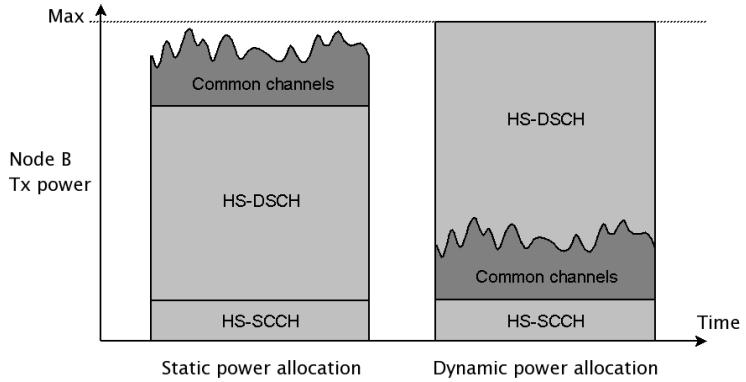

FIGURE 9 Power allocation with static and dynamic HSDPA power allocation (fixed HS-SCCH power).

Admission control

As HSDPA is a shared channel concept, its admission control differs from Release '99 decicated channel admission control. As different services do not coexist at the same TTI in the cell, new admission control algorithms are needed to decide the acceptance of a new call request but at the same time to ensure adequate transmission quality to existing users.

RNC uses Node B and UE measurements and parameters to make the decision for the new call request. These parameters and measurements are:

- total average Tx power of the cell,
- non-HSDPA Tx power of the cell,

- HS-DSCH power needed to serve the HSDPA users,
- guaranteed bit rates of HSDPA users,
- requesting user pilot level,
- new user QoS attributes.

From these parameters RNC can estimate if the cell has enough available HSDPA capacity to ensure the QoS for all users if a new call is accepted.

2.3.8 Mobility management

HSDPA transmission for a UE takes place in only one cell at a time. This cell is called the serving HS-DSCH cell. The cell is selected by the RNC from the UEs active set. No active set changes or updates are necessary for HSDPA operation. The HSDPA transmission in a UE is totally independent of the cell connection states of the DCH.

The RNC is responsible for changing the serving HS-DSCH sector according to the UE measurements of the CPICH levels of the sectors in the active set. The handoff can also be triggered by Node B if the measurements show degradation in uplink quality. This is done in order to ensure reliable reception of CQI and ACK/NACK messages in HS-DPCCH.

Fig. 10 presents the basic functionality of serving HS-DSCH sector change in HSDPA triggered by the UEs measurements of the E_c/I_o levels or the received signal code power (RSCP) levels of the cells in the UEs active set. When another active set sector pilot becomes stronger than the current serving HS-DSCH sector pilot plus the hysteresis value, the RNC starts a handover timer. The hysteresis is used to avoid a "ping pong" effect in handovers and also to specify a cell individual offset (CIO) to favour certain cells in order to extend their HSDPA coverage in some scenarios.

If the pilot of the new cell stays stronger than the pilot of the current HS-DSCH cell plus the hysteresis value for a time duration equal to "time-to-trigger", the handover is initiated.

HSDPA supports both intra Node B and inter Node B handover procedure. In intra cell handover there is a minimal interruption in data flow. The HARQ process functionality stays uninterrupted. It means that every packet from the old cell MAC-hs is moved to the new cell MAC-hs without any need for higher layer retransmissions.

In inter Node B handover, the terminal flushes all the buffers and starts to listen to the new base station. Also Node B flushes all the packets in its buffers, including all unfinished HARQ processes, belonging to the UE that is handed off. RLC layer retransmissions are needed for the lost packets during the handover delay if the RLC acknowledged mode is used. In unacknowledged mode there are no RLC retransmissions. In order to minimize the packet loss in the RLC unacknowledged mode during the cell change the RNC can calculate accurately the exact time of the handover and restrain in sending packets at the very

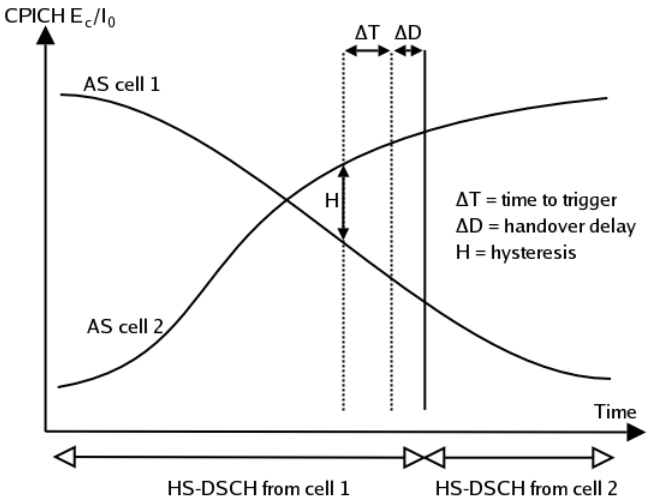

FIGURE 10 HS-DSCH serving sector handover functionality.

last moment to the serving HS-DSCH cell being replaced. To minimize possible further data loss the support of out-of-sequence PDUs was introduced in RLC unacknowledged mode in Release 6 allowing the UTRAN to bi-cast the packets to both the old and new serving HS-DSCH cells during the handover.

3 RECEIVER STRUCTURES

In this chapter the UE reception algorithms are addressed. First the basics of multipath radio channels are presented in chapter 3.1. The conventional rake receiver structure and the mathematical modeling of it in the system simulator is covered in chapter 3.2. The problems with intra- and inter-cell interference is explained in chapters 3.3 and 3.4, respectively. As a solution to mitigate these, an advanced UE reception algorithm, linear minimum mean squared error (LMMSE) chip-level equalizer and its modeling issues are presented in chapter 3.5. More information on advanced receiver structures can be found e.g. in [Lat99].

3.1 Multipath radio channels

Different reflections, diffractions and attenuation of the transmitted signal energy caused by natural obstacles such as buildings and land forms characterize the terrestrial radio channel. The same signal energy may arrive at the receiver via multiple different paths at different time instants. This phenomenon defines the multipath power delay profile of the channel. The profile represents a sort of temporal impulse response of the channel, i.e. the impact of the channel to a signal sent in one symbol time. The received replicas of the same transmitted signal at different time instants are called taps.

Two example channel power delay profiles used in the simulations of this thesis are presented in Table 5. The profiles are modified versions of Pedestrian A (PedA) and Vehicular A (VehA) models presented originally by the International Telecommunication Union Radiocommunication Sector (ITU-R) in [ITU97]. For the sake of modeling and notational simplicity the profiles are modified so that the delays match integer chips.

Fig. 11 depicts two different channel types, a frequency selective and a flat fading channel. Multipath propagation has an effect on the frequency response of the channel. From the power delay profiles of VehA and PedA it can be seen that VehA represents a rich scattering environment with several multipaths. This

leads to a frequency-selective channel. PedA has a strong tap at zero delay and only one other weak path. Thus, PedA is more a flat-fading channel.

TABLE 5 Channel profile power delay profiles.

Channel profile	Path delays [slots]					
VehA	0	1	3	4	7	10
PedA	0	1				
	Path powers [dB]					
VehA	-3.1	-5.0	-10.4	-13.4	-13.9	-20.4
PedA	-0.2	-13.5				

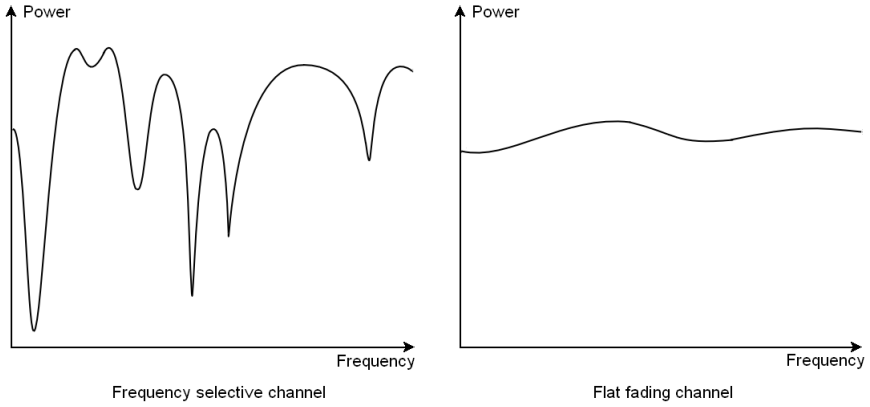

FIGURE 11 Frequency selective and flat fading radio channels.

The taps are detected by sampling the channel at regular intervals. The maximum sampling interval of the WCDMA receiver is the chip duration. When using oversampling the receiver samples the channel more than once during a single chip duration. In this thesis no oversampling is assumed. Fig. 12 presents a multipath radio channel profile where the second and the third tap arrive at the receiver within the same chip-time. Without oversampling the WCDMA receiver cannot distinguish them and their energy is combined to form a single tap. If the tap phases are different, they can be combined destructively. This effect manifests itself as signal cancellation called fast fading.

The occurrence of fast fading is dependent on the lengths of the signal paths. If two signal paths have a length difference of more than 78 meters (= speed of light $\div$ chip rate = 3.0×10^8 m/s $\div$ 3.84 Mcps), they arrive at the receiver at two different chip-times and can be separated. If the path length difference is shorter, they arrive at the same chip duration and are seen as single tap, if they do not cancel each other out.

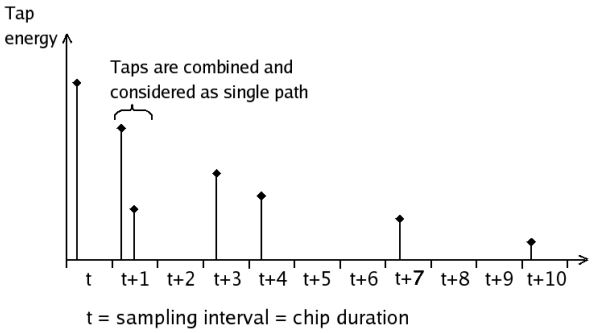

FIGURE 12 Example of a multipath radio channel.

3.1.1 Mathematical modeling of multipath radio channel

If it is assumed that there exists N_{Rx} Rx-antennas at UE the received chip sequence $\mathbf{y}$ equals

$$\mathbf{y} = \mathbf{H}^T\mathbf{x} + \mathbf{n}\,, \tag{4}$$

where $\mathbf{H}$ is the channel matrix between the transmitter and the receiver and the transmitted chip stream $\mathbf{x}$ is

$$\mathbf{x} = [x[t+F+L-D]\cdots x[t]\cdots x[t-D]]^T \tag{5}$$

and $\mathbf{n}$ is the noise vector consisting of the both the neighboring sector interference and the thermal noise over the bandwidth. Here F is the length of the linear filter, which models the receiver. The calculation of filter coefficients is discussed in chapter 3. D is the delay parameter satisfying $(0 \leq D \leq F)$ and L is the delay spread of the channel normalized to the chip interval. Multiplication by the $(F+L)\times(F\times N_{Rx})$ channel coefficient matrix $\mathbf{H}$ in Eq. 4 models the convolution between the transmitted chips and the impulse response of the channel. Thus,

$$\mathbf{H} = \begin{bmatrix} \mathbf{h}_{N_{Rx}\times(L+1)} & \mathbf{0}_{N_{Rx}\times 1} & \cdots & \mathbf{0}_{N_{Rx}\times 1} \\ \mathbf{0}_{N_{Rx}\times 1} & \mathbf{h}_{N_{Rx}\times(L+1)} & \cdots & \vdots \\ \vdots & \vdots & \ddots & \mathbf{0}_{N_{Rx}\times 1} \\ \mathbf{0}_{N_{Rx}\times 1} & \mathbf{0}_{N_{Rx}\times 1} & \mathbf{0}_{N_{Rx}\times 1} & \mathbf{h}_{N_{Rx}\times(L+1)} \end{bmatrix}^T, \tag{6}$$

where $\mathbf{h}$ is the $N_{Rx}\times(L+1)$ channel impulse response matrix defined by

$$\mathbf{h} = \begin{bmatrix} h_1[0] & h_1[1] & \cdots & h_1[L] \\ h_2[0] & h_2[1] & \cdots & h_2[L] \\ \vdots & \vdots & \ddots & \vdots \\ h_{N_{Rx}}[0] & h_{N_{Rx}}[1] & \cdots & h_{N_{Rx}}[L] \end{bmatrix}, \tag{7}$$

where $h_i[l]$ is the channel impulse of i^{th} Rx-antenna at delay l.

Signal reception

Using the signal model presented in chapter 3.1.1 the receiver can be defined with a $F \times N_{Rx}$ chips long linear filter $\mathbf{w}$ which is used to obtain the chip estimate $\tilde{\mathbf{x}}$ for the transmitted chip sequence $\mathbf{x}$ i.e.

$$\tilde{\mathbf{x}} = \mathbf{w}^T \mathbf{y} \,. \tag{8}$$

The signal-to-interference and noise ratio at the output of a linear filter may then be calculated by evaluating the power of the specific signal and noise terms after the filtering as in [Kom00, Luc03]. These methods can directly be applied when calculating the signal to interference and noise ratio (SINR) at the output of the linear receiver. Thus,

$$\text{SINR} = \frac{S_f P_{ch} |\mathbf{w}^T \mathbf{H}^T \delta_D|^2}{P_{tot} \mathbf{w}^T \mathbf{H}^T \hat{\delta}_D \hat{\delta}_D^T \mathbf{H}^* \mathbf{w}^* + \mathbf{w}^T \mathbf{C}_w \mathbf{w}^*} \,, \tag{9}$$

where S_f is the channel spreading factor, P_{ch} is the channel transmit power and P_{tot} is the total transmit power of the sector and

$$\delta_D = \begin{bmatrix} 0 & \cdots & 0 & 1 & 0 & \cdots & 0 \end{bmatrix}^T \,, \tag{10}$$

which represents the delay of the equalizer. The left-most term in the divisor models the intra-cell interference (i.e. inter-path interference) and right-most term models the inter-cell interference and background noise. SINR is calculated according to Eq. 9 for all linear receivers and the definition of $\mathbf{w}$ varies according to the linear receiver type used. Moreover, in Eq. 9 $\hat{\delta}_D$ is a $(F \times F)$ matrix defined by

$$\hat{\delta}_D = diag(\begin{bmatrix} 1 & \cdots & 1 & 0 & 1 & \cdots & 1 \end{bmatrix}) \tag{11}$$

and it is used in the matrix product $\mathbf{H}^T \hat{\delta}_D \hat{\delta}_D^T \mathbf{H}^*$ to extract the elements from the channel matrix that are used in the inter-path interference calculation.

In Eq. 9 the $(F \times N_{Rx}) \times (F \times N_{Rx})$ interference matrix

$$\mathbf{C}_w = \begin{bmatrix} \sigma_1^2 & 0 & 0 & 0 & 0 & 0 \\ 0 & \ddots & 0 & 0 & 0 & 0 \\ 0 & 0 & \sigma_{N_{Rx}}^2 & 0 & 0 & 0 \\ 0 & 0 & 0 & \sigma_1^2 & 0 & 0 \\ 0 & 0 & 0 & 0 & \ddots & 0 \\ 0 & 0 & 0 & 0 & 0 & \sigma_{N_{Rx}}^2 \end{bmatrix} \,, \tag{12}$$

where

$$\sigma_j^2 = I_{tot}^j - I_i^j \,, \tag{13}$$

if the interference is assumed to be uncorrelated between the receive antennas. The antenna-wise total downlink interference from all sectors to UE in Eq. 13 is calculated as

$$I_{tot}^j = \sum_{i=1}^{k} I_i^j + N_0 \,, \tag{14}$$

where k is the number of sectors in the simulation area and N_0 is thermal noise. Finally, the downlink interference from one sector to observed UE is calculated as

$$I_i^j = P_i L_i \sum_{l=1}^{N_i} (g_{i,l} \| h_{i,l}^j \|^2), \tag{15}$$

where P_i is the downlink transmission power in the sector i and L_i is the slow faded path loss between the UE and sector i. N_i is the number of multipath components provided by the simulated environment in sector i, $g_{i,l}$ is the average path gain of the l^{th} component and $h_{i,l}^j$ is complex channel coefficient for sector i, multipath component l and receive antenna j.

3.2 Rake receiver

If several taps arrive at the receiver more than one chip-time apart, these signals can be separated and combined coherently in WCDMA. This is called multipath diversity. Using the rake reception algorithm the multipaths can be combined and multipath diversity obtained. The phases of rake reception algorithm is described shortly in the following [Hol04].

1. Received taps are identified from the signal.
2. Correlation receivers, a.k.a. rake fingers are allocated to each tap.
3. Phase shift induced by the channel for each finger is tracked using a channel estimation formed from the pilot symbol
4. Phase shifts are reversed.
5. Fingers are combined coherently.

The presented signal combining algorithm is also called Maximum Ratio Combining (MRC). A block diagram of example three finger rake receiver is presented in Fig. 13. Digitized input samples are received in the form of I and Q branches. Code generators and a correlator perform the despreading and integration to user data symbols. The phase rotator removes the channel effect to the received fingers with the channel estimate provided by the channel estimator. The delay is compensated by the difference in arrival times of the symbols in each finger. The channel compensated symbols are then combined by the rake combiner thereby providing multipath diversity against fading. The matched filter is used for determining and updating the current multipath delay profile of the channel. This measured delay profile is then used to assign the rake fingers to the largest peaks [Hol04].

Multiple receive antennas can be applied by just adding additional rake fingers to the antennas. This is the same as multiple paths received from a single antenna. Thus, all the energy from multiple paths and antennas can be received.

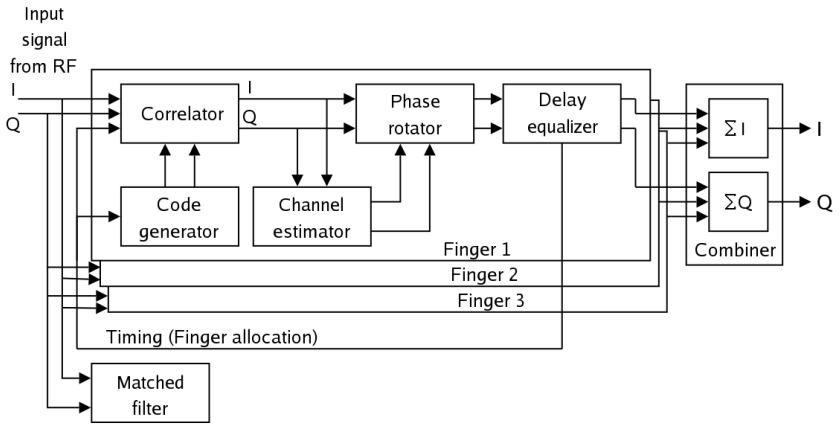

FIGURE 13 Rake receiver block diagram [Hol04].

From the receiver's perspective, there is no essential difference between these two forms of diversity reception.

3.2.1 Modeling of rake by linear filtering

For the rake receiver the linear filter coefficient vector $\mathbf{w}$ contains the rake combiner coefficients. In other words, the order of despreading and combining is reversed to typical order of combining despread symbols i.e. $\mathbf{w}$ with N_{Rx} receive antennas consists of conjugated channel coefficients (which are assumed to be ideally known on the system level) and it can be written as

$$\mathbf{w}_{\text{rake}} = \mathbf{H}^H \delta_D \,. \tag{16}$$

3.3 Intra-cell interference

In WCDMA orthogonal Walsh-Hadamard spreading sequences are used to separate the downlink channels from each other. Signals being orthogonal mean that they are fully separated and can be received separately without any interference to another like they were sent with different frequencies or times.

A bad feature of the orthogonal spreading sequences is that they have a high cross-correlation with the delayed versions of themselves. This becomes a problem if a data spread with code c_1 at time instant t_1 and another data spread with code c_2 at time instant t_2 is received at the same time instant t_3. Since the transmission time instances of the two data are different, their spreading codes are not fully orthogonal and the transmissions interfere with each other. This type of interference eminating from the serving cell is called intra-cell interference or Multiple Access Interference (MAI).

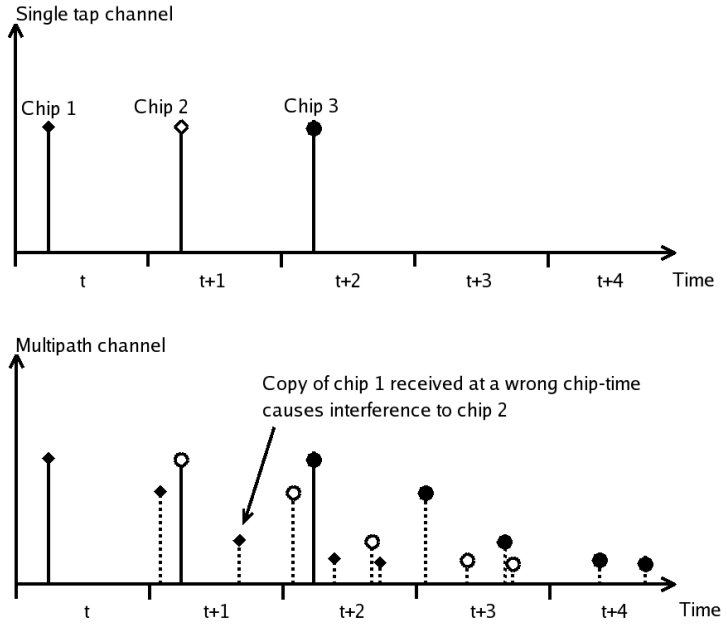

FIGURE 14 Multiple access interference.

Fig. 14 presents the occurrence of MAI caused by the multipath propagation of the own channel signal. Although rake receiver can exploit the multipath diversity by finding and combining taps of the same transmission arriving at the receiver during several chip-times, the delayed versions of the desired signal cause interference at the same time. Other channels transmitted by the serving cell interfere the signal as well but are not depicted in the figure. The problem of compromised orthogonality of the spreading codes occurs only in frequency-selective channels, where several taps are received more than one chip-time apart. In a flat-fading channel only a single tap arrives at the receiver, i.e. a sent signal is received only once. Therefore, a similar problem with the signal delays does not exist and the channels remain orthogonal. However, frequency-selective channels where MAI is a problem are very common in WCDMA networks and thus advanced algorithms targeting to mitigate intra-cell interference are beneficial.

3.4 Inter-cell interference

The different scrambling codes, channel states and angles-of-arrivals (AOA) of the neighboring base station signals affect the characteristics of the inter-cell interference, which is dominant in cell border regions. The long scrambling codes that are used to separate different base station signals are not orthogonal. Thus, inter-cell interference is present regardless of the delay profile of the radio chan-

nel, unlike intra-cell interference, which is present only in frequency-selective channels. Due to the different nature of the inter-cell interference, mitigating it by employing same methods than with intra-cell interference is not possible. However, any interference can be suppressed from the signal if its effect can be estimated. Thus, by estimating the interfering neighboring sector signals based on their characteristics they also can be mitigated.

3.5 Linear MMSE chip-level equalizer

One option to mitigate the effect of MAI is to use chip-level equalization of the channel. Linear Minimum Mean Squared Error (LMMSE) chip-level equalizer can be used in frequency-selective channels to make the channel flat again and restore the orthogonality lost due to time-shifts between the signals. A block diagram of the general signal reception with channel equalization is presented in Fig. 15. The received chip sequence $\mathbf{y}$ is basically the sent signal $\mathbf{x}$ influenced by the channel $\mathbf{h}$. Equalizer takes $\mathbf{y}$ as an input and uses it and the channel estimate $\tilde{\mathbf{h}}$ to form an estimate $\tilde{\mathbf{x}}$ of the original sent signal. This estimate is then used in despreading.

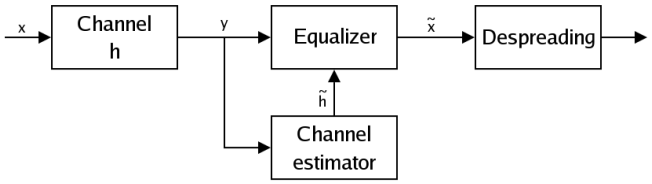

FIGURE 15 Block diagram of signal reception with channel equalization.

The benefit of LMMSE chip-level equalization is its simplicity and good performance in frequency-selective channels. However the complexity of the equalizer is dependent on the delay spread of the channel. In channels with a larger delay spread a much longer and thus more complex equalizer is needed. The length of the delay spread is the limiting factor for the use of a chip-level equalizer in practice [Hoo03].

3.5.1 Modeling of equalizer by linear filtering

Chip-level equalization utilizes the channel information and MMSE criterion in order to form a synchronized multi-user chip estimate prior to despreading. As a by-product, the orthogonality between the channels which was lost due to dispersive channel is restored and hence, MAI is mitigated. After the chip-level equalizer, the overall channel (convolution of the channel $\mathbf{H}$ and the equalizer filter $\mathbf{w}$) should be frequency non-selective again with 1 tap only.

If the LMMSE solution in [Kra00a, Kra00b] is applied, the equalizer coefficient vector is

$$\mathbf{w}_{\text{LMMSE}} = \mathbf{C}_w^{-1}\mathbf{H}^H(\mathbf{H}\mathbf{C}_w^{-1}\mathbf{H}^H + \mathbf{I})^{-1}\delta_D\,. \tag{17}$$

Note that delay can be optimized for LMMSE as in [Kra00a].

3.5.2 Interference aware equalizer

With the signal model presented in Eq. 4 only the own sector channel is assumed to be known and thus the equalizer is able to mitigate only the intra-cell interference. Due to the random scrambling codes used at the interfering base stations the inter-cell interference is assumed as white Gaussian noise having a known variance at the receiver.

With interference aware equalizer, the channels between the UE and its strongest interfering sectors (which give the highest contribution to inter-cell interference seen by the UE) are assumed to be known. Thus, the channel matrices for those sectors are constructed also and the received signal is filtered with equalizer coefficients. Note that sector index j in Eq. 18-21 and in Eq. 25-26 represents how strong the interference power from UE point of view is, i.e. the lower the index, the stronger the interference power. Hence, indexes between $[1, N_{\text{IBS}}]$ refer to the strongest interfering base stations (sectors) taken into account. Sectors with indexes between $[N_{\text{IBS}}+1, k]$ assume white interference model, where k is the total number of sectors in the simulation area. Thus, the signal model with the partially colored inter-cell interference becomes

$$\mathbf{y} = \mathbf{H}^T\mathbf{x} + \sum_{j=1}^{N_{\text{IBS}}}\left(\mathbf{H}_j^T\mathbf{x}_j\right) + \mathbf{n}\,, \tag{18}$$

where $\mathbf{H}_j$ and $\mathbf{x}_j$ are the channel matrix and the transmitted bit sequence of the interfering base station j, respectively.

Linear filter coefficients

With interference aware LMMSE equalizer (I-LMMSE) the linear filter coefficient vector $\mathbf{w}$ is calculated using the inverse of the covariance matrix $\mathbf{C}_{\text{rr}}$.

$$\mathbf{w}_{\text{I-LMMSE}} = \mathbf{C}_{\text{rr}}^{-1}\mathbf{M}^H\delta_D\,, \tag{19}$$

where the $(FN_{Rx}) \times (F+L)$ matrix $\mathbf{M}$ is defined by

$$\mathbf{M} = \begin{bmatrix} \mathbf{H}_1^H \\ \vdots \\ \mathbf{H}_{N_{Rx}}^H \end{bmatrix}, \tag{20}$$

where $\mathbf{H}_i$ is the own sector channel matrix from receive antenna i. Matrix $\mathbf{M}$ for the interfering base stations can be constructed correspondingly. The $(FN_{Rx}) \times (FN_{Rx})$ covariance matrix $\mathbf{C}_{\text{rr}}$ is defined as

$$\mathbf{C}_{\text{rr}} = P_{tot}\mathbf{M}\mathbf{M}^H + \sum_{j=1}^{N_{\text{IBS}}} P_{tot,j}\mathbf{M}_j\mathbf{M}_j^H + \sigma^2\mathbf{I}, \tag{21}$$

where P_{tot} and $P_{tot,j}$ are the total Tx powers of the serving sector and interfering sector j, respectively. The white noise interference term

$$\sigma^2\mathbf{I} = \begin{bmatrix} I_1 & \dots & 0 \\ 0 & \ddots & 0 \\ \vdots & 0 & I_{N_{Rx}} \end{bmatrix}, \tag{22}$$

where $\mathbf{I}_i$ is the $F \times F$ white noise interference matrix of receive antenna i defined by

$$\mathbf{I}_i = \begin{bmatrix} \sigma_i^2 & \dots & 0 \\ 0 & \ddots & 0 \\ \vdots & 0 & \sigma_i^2 \end{bmatrix}, \tag{23}$$

where σ_i^2 is the noise power of receive antenna i.

SINR calculation

The SINR calculation using white inter-cell interference was presented in Eq. 9. Extension to colored noise can be derived from Eq. 18:

$$\text{SINR} = \frac{P_{ch}\left|\mathbf{w}^T\mathbf{H}^T\delta_D\right|^2}{P_{tot}\mathbf{w}^T\mathbf{H}^T\hat{\delta}_D\hat{\delta}_D^T\mathbf{H}^*\mathbf{w}^* + I_{\text{color}} + \mathbf{w}^T\mathbf{C}_w\mathbf{w}^*}, \tag{24}$$

where I_{color} is the colored interference of N_{IBS} strongest base stations and is defined as

$$I_{\text{color}} = \sum_{j=1}^{N_{\text{IBS}}} P_{tot,j}\mathbf{w}^T\mathbf{H}_j^T\mathbf{H}_j^*\mathbf{w}^*. \tag{25}$$

The interference matrix $\mathbf{C}_w$ is otherwise similar to that in Eq. 12 but with this model the sectors which interference is calculated explicitly are removed from the white noise term as their contribution to inter-cell interference is modeled realistically. Thus, the calculation of total downlink interference to UE antenna i from all sectors which interference is assumed white is now defined by

$$I_{\text{tot}}^i = \sum_{j=1+N_{\text{IBS}}}^{k} I_j^i + N_0, \tag{26}$$

where k is the number of sectors in the simulation area and N_0 is thermal noise.

4 ANTENNA DIVERSITY

Signal fading causes such large problems in wireless systems that the dependence of just a single signal path can lead to significant performance degradation. One option to mitigate the effect of signal fading is to use repetition in time domain. This is a sort of insurance in case the channel is in a bad condition at the time of signal transmission. By transmitting the signal also another time decreases the probability that the signal is totally lost. If one signal is lost, there still exists a copy or copies of the same signal and the signal can be recovered. Repetition of the signal in time is called time diversity.

If the data transmission is very delay sensitive, it might not be possible to use time diversity because the transmission of identical copies of the same signal decreases the transmission rate of the new data. Therefore there is a need for alternative method to achieve the same diversity order but not at the cost of the data rate. One option to achieve this is to use spatial diversity, i.e. to transmit and receive multiple copies of the same data at the same time in different locations.

The way to achieve spatial diversity in wireless systems is to use multiple transmit and receive antennas. Channel fading is dependent on the spatial attributes of the signal path between a transmit antenna and receive antenna. If antennas are located sufficiently far apart and there are enough differences in the scattering environment of the transmitted signals, each of them fades independently. Thus, it is beneficial to offer multiple transmission paths to the signal in order to combine more or less deteriorated signal copies at the receiver to form one sufficiently good signal.

The order of diversity is dependent on the amount of transmit antennas N_{Tx} and receive antennas N_{Rx} so that the diversity order is $N_{Tx} \times N_{Rx}$. When solely receive diversity is used, the scheme is referred to in this thesis as $1 \times N_{Rx}$ scheme, where $N_{Rx} > 1$. A scheme with mere transmit diversity is referred correspondingly $N_{Tx} \times 1$. A scheme which employs both receive and transmit antenna diversity ($N_{Tx} \times N_{Rx}$) provides additional gain to $1 \times N_{Rx}$ and $N_{Tx} \times 1$ schemes. As there are significant differences between utilization of transmit and receive antenna diversity, they will be discussed separately.

Fig. 16 presents the antenna diversity cases studied in this thesis. Maximum

of two transmit or receive antennas are considered.

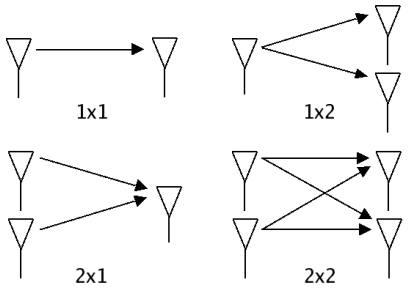

FIGURE 16 Studied transmit and receive antenna scenarios.

Transmit diversity techniques can further divide into single and multiple stream techniques. This thesis considers single and dual stream closed loop transmit diversity techniques, single and dual stream TxAA. D-TxAA is the chosen Multiple Input - Multiple Output technique for HSDPA in 3GPP specification release 7.

4.1 Receive diversity

Multiple receive antennas can be implemented both in the base station and in the UE in order to capture spatial receive diversity. In the base station Rx diversity can easily be utilized to improve uplink capacity and coverage. However, receive diversity in the user equipment has been traditionally considered troublesome due to cost and space issues. Nevertheless, Rx diversity is one of the most efficient diversity techniques and therefore a very intriguing option to improve data transmission in the downlink.

In a system exploiting N_{Rx} antennas at the receiver ($N_{Rx} > 1$), the received signal vector at time instant t can be noted as

$$\begin{bmatrix} y_1[t] \\ \vdots \\ y_{N_{Rx}}[t] \end{bmatrix} = \begin{bmatrix} h_1[t] \\ \vdots \\ h_{N_{Rx}}[t] \end{bmatrix} x[t] + \begin{bmatrix} n_1[t] \\ \vdots \\ n_{N_{Rx}}[t] \end{bmatrix}, \tag{27}$$

where x is the transmitted signal, h_i and n_i are the channel and the noise between transmit antenna and receive antenna i. In other words, we receive N_{Rx} replicas of the sent signal x and we can detect it from $y_1, \ldots, y_{N_{Rx}}$.

Two types of gain are achieved in this kind of system, assuming that the spatial characteristics of the paths from the transmit antenna to the receive antennas differ sufficiently, resulting in N_{Rx} independent channels. The first gain is a power gain which in theory grows linearly according to N_{Rx}. Power gain is

achieved because of the fact that the one sent signal energy is received by N_{Rx} antennas and the received powers can be combined.

Another gain is diversity gain. This gain comes from the assumption that the transmitted signal fades independently in every path between the transmit antenna and N_{Rx} receive antennas. This leads to decreased probability that the overall received signal gain is low.

However, the diversity gain is only applicable when all the N_{Rx} signal paths fade independently. If the paths are completely correlated, then only the power gain is achieved with receive diversity.

4.2 Transmit diversity

The utilization of transmit diversity mainly increases the transmitter complexity without the need for drastic hardware changes at the receiver. Hence, a significant effort has been devoted in 3GPP to develop efficient transmit diversity solutions to enhance downlink capacity.

When N_{Tx} transmit antennas ($N_{Tx} > 1$) and only one receive antenna is used, the situation is more complicated than in a mere receive diversity scheme. One can't just transmit the same signal at the same time from all transmit antennas although all the signal paths would fade independently. Due to the fact that the antennas share the base station power, the transmitted signals have $1/N_{Tx}$ of the power of the base station and thus no power gain would be attained at the receiver.

Diversity gain can be attained with transmit diversity by transmitting the same symbol at different times from different antennas. This means that only one antenna transmits at a time instance and the rest are silent. This however is mere repetition and does not utilize the whole potential of the additional transmit antennas. As it is not feasible to send the same symbol at the same time instant from several antennas, the gain of multiple antennas can be achieved by sending more than one symbol at a time.

When using two transmit antennas, space-time block codes can be used to achieve gain over mere time diversity without any knowledge of the channel. Additionally, when the channel state information is present, transmit diversity can provide quite significant gains over one branch transmission.

4.2.1 Space time transmit diversity (STTD)

The simplest and probably the most known space-time block coding scheme is the Alamouti scheme [Ala98] or space time transmit diversity (STTD) which support is mandatory for the UE in UMTS [3G05]. The block diagram of STTD operation with single receiver antenna is presented in Fig. 17.

STTD operation can be summarized as follows ([Ala98], [Tse05], [Hot03]). In STTD two symbols x_1 and x_2 are sent at one symbol period over antennas 1 and

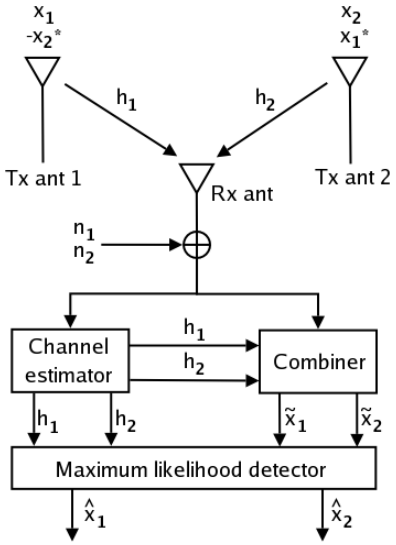

FIGURE 17 STTD transmit diversity operation block diagram [Ala98].

2, respectively. The same symbols are sent again in the next symbol period but they are coded so that they are orthogonal at the receiver and can be combined with the symbols received during the first period thus achieving both diversity and power gain. At time instant 2, antenna 1 sends $-x_2^*$ and antenna 2 sends x_1^*. Let's assume that the channels remain constant over two symbols periods, i.e. $h_i = h_i[1] = h_i[2], i = 1, 2$. The received signal y at time instants 1 and 2 can be written as

$$\begin{bmatrix} y[1] \\ y[2] \end{bmatrix} = \frac{1}{\sqrt{2}} \begin{bmatrix} x_1 h_1 + x_2 h_2 \\ x_1^* h_2 - x_2^* h_1 \end{bmatrix} + \begin{bmatrix} n[1] \\ n[2] \end{bmatrix}, \tag{28}$$

where h_i represents the channel gain from transmit antenna i to receive antenna and n is the noise. The received symbol matrix is normalized by $\frac{1}{\sqrt{2}}$ so that the same power is used for STTD transmission as would be used if the symbols were independently transmitted from one antenna. Conjugating the received signal during the second symbol period the received signal equation can be written as

$$\begin{bmatrix} y[1] \\ y[2]^* \end{bmatrix} = \mathbf{H} \begin{bmatrix} x_1 \\ x_2 \end{bmatrix} + \begin{bmatrix} n[1] \\ n[2]^* \end{bmatrix}, \tag{29}$$

where

$$\mathbf{H} = \frac{1}{\sqrt{2}} \begin{bmatrix} h_1 & h_2 \\ h_2^* & -h_1^* \end{bmatrix}. \tag{30}$$

The space-time matched filtering proceeds by applying the Hermitian conjugate $\mathbf{H}$ on the received signal:

$$\mathbf{H}^H \begin{bmatrix} y[1] \\ y[2]^* \end{bmatrix} = \begin{bmatrix} \tilde{x}_1 \\ \tilde{x}_2 \end{bmatrix} = \frac{1}{2}\left(|h_1|^2 + |h_2|^2\right) \begin{bmatrix} x_1 \\ x_2 \end{bmatrix} + \begin{bmatrix} n[1] \\ n[2]^* \end{bmatrix} \tag{31}$$

By employing space-time block coding the transmitted symbols pass through orthogonal channels which do not interfere with each other. Thus, the energy used on the symbols during two transmit periods can be combined forming space-time matched filter soft outputs $\tilde{x}_1$ and $\tilde{x}_2$. They can then be used as input for the hard decision maker e.g. maximum likelihood sequence detector which ultimately forms the transmitted symbol estimates $\hat{x}_1$ and $\hat{x}_2$.

As the transmit power is divided into two symbols, we do not get the similar power gain as in receive diversity, where the received power was linearly dependent on the number of receive antennas. Using STTD we get power gain over repetition coding as lower power is needed per symbol.

Channel model and SINR calculation with STTD

STTD operation changes the channel coefficient matrix definition of the general signal model presented in chapter 3.1.1. As two transmit antennas are used and two separate signals are transmitted, they have to be taken into account. Hence, the channel matrix definition becomes

$$\mathbf{H} = \begin{bmatrix} \mathbf{H}_1 \\ \mathbf{H}_2 \end{bmatrix}. \tag{32}$$

Two receiver filters $\mathbf{w}_1$ and $\mathbf{w}_2$ are used in computing separately the two SINRs, noted as S_1/I_1 and S_2/I_2. Filters are defined similarly for both Rake and LMMSE equalizer as defined in chapter 3. After STTD decoding, only one SINR is obtained.

The form of instantaneous SINR of antenna i has the form

$$\frac{S_i}{I_i} = \frac{S_f P_{HS-DSCH} |\mathbf{w}_i^T \mathbf{H}_i^T \delta_D|^2}{\underbrace{|\mathbf{w}_i^T \mathbf{H}_i^T \hat{\delta}_D|^2}_{I_{intra}} + \underbrace{|\mathbf{w}_i^T \mathbf{H}_j^T \hat{\delta}_D|^2}_{I_j} + \underbrace{\mathbf{w}_i^T \sigma_n^2 \mathbf{w}_i^*}_{I_{inter}}}, \tag{33}$$

where $j = 2$ when $i = 1$ and vice versa, S_f is the spreading factor, $P_{HS\text{-}DSCH}$ is the HS-DSCH transmit power, I_{intra} is the intra-cell interference and I_j is the interference from antenna j. I_{inter} is the inter-cell interference consisting of neighboring cell interference and also the system noise.

We denote the convolution between the channel coefficients $(c_i, i = 1,2)$ and the filter coefficients $(\mathbf{w}_i, i = 1,2)$ with a_1 and a_2, having the form of $a_i = c_i \otimes \mathbf{w}_i, i = 1,2$, where $\otimes$ denotes the convolution operation. The final SINR after decoding contains the contribution of antenna 1 weighted by a_1 and also the contribution of antenna 2 weighted by a_2. Thus, the ratio between the signal component S and the interference component I will express the final SINR.

An intuitive form of the received signal might be expressed as

$$r = a_1(\sqrt{S_1}x + n_1) + a_2(\sqrt{S_2}x + n_2), \tag{34}$$

where x is the amplitude of the combined received signal, n_1 and n_2 are the corresponding noise levels and i is the Tx antenna index. Due to the coherent combining of the signal components S_1 and S_2 and also due to the non-coherent combining of the interference component I_1 and I_2, the SINR is expressed as

$$SINR = \frac{S}{I} = \frac{(a_1\sqrt{S_1} + a_2\sqrt{S_2})^2}{a_1^2 I_1 + a_2^2 I_2}. \tag{35}$$

4.2.2 Closed loop transmit diversity

Channel state information (CSI) can be utilized effectively if it is known at the transmitter before transmission. By knowing the effect of the channel to transmitted signal it can be reduced or even canceled. However, to achieve CSI the transmitter needs constant feedback from the receiving entity.

Generally, in closed loop transmit diversity (CLTD) a signal is transmitted during one symbol period from all transmit antennas. The phases of the signals sent from each antenna are weighted according to the receiver feedback in order to exploit the phase shift caused by the channel and to turn its effect in favor.

When the expected phase shift is known the sent signal phases can be altered the way that all sent signals arrive at the receiver in-phase and thus they can be combined constructively. The form of the received signal y at time instant t can be written as

$$y[t] = \left(\sum_{i=1}^{N_{Tx}} w_i[t] h_i[t] \right) x[t] + n[t], \tag{36}$$

where $w_i[t]$ is the applied complex weight and $h_i[t]$ is the channel impact between the receiver and transmit antenna i at time instant t. In this thesis only the two transmit antenna scheme is considered. When two transmit antennas are used the weight applied to antenna 1 remains constant and only the phase of the second antenna is altered. Ideally, weight w_2 should be selected so that the phases of $w_1[t]h_1[t]$ and $w_2[t]h_2[t]$ are the same.

The correct behavior of closed loop transmit diversity demands that the channel state information is correct and up to date. Many phenomenons degrade the performance of CLTD. Firstly, feedback is subject to errors due to uplink channel imperfections. Incorrect feedback results in incorrect phase shifts of the second signal and the received signals can be combined destructively at the receiver. Also, there is a delay between the measurement of the channel in the receiver and the usage of the CSI. If the channel changes rapidly, the CSI is not up to date and becomes useless. Therefore, the coherence time of the channel must be longer than the feedback delay. Closed loop transmit diversity might not give gain with high mobile velocities due to rapid channel variations.

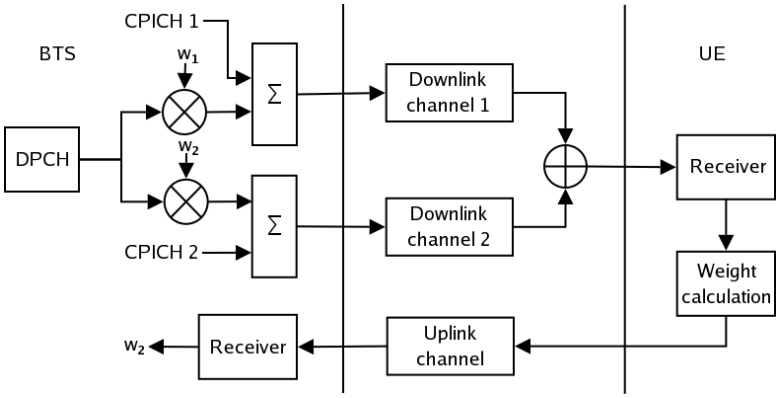

FIGURE 18 Single stream TxAA operation block diagram [3G04a].

4.2.3 Single stream Transmit Antenna Array (TxAA)

Single stream TxAA (or Closed Loop Mode 1) operation block diagram for two transmit antennas is presented in Fig. 18. There the transmitted pilot signals from antennas 1 and 2 are weighted with the antenna specific weighting factor w_1 and w_2, respectively. The signals pass through multipath fading downlink channel. The receiving entity calculates the optimal factor w_2 for transmit antenna 2 from the received signals. The weight is then sent to the transmitter. As there are only a limited amount of feedback bits available to be used in realistic implementations of CLTD, the amount of phase rotation possibilities is also limited. In TxAA the weight for antenna 1 is constant $1/\sqrt{2}$ and for antenna 2 the weight w_2 used in slot $t+1$ is calculated from two consecutive feedback bits sent by the UE so that

$$w_2[t+1] = 1/\sqrt{2}e^{j\phi[t]}\,, \tag{37}$$

where

$$\phi[t] = \arg(j^{t \bmod 2}\,\mathrm{sgn}(y[t]) + j^{(t-1) \bmod 2}\,\mathrm{sgn}(y[t-1]))\,, \tag{38}$$

where $y[t]$ is the feedback command received in slot t [Hot03]. The sign function in Eq. 38 is used to quantize each received feedback bit. Simplified, each feedback bit represents either the real or the imaginary part of the feedback weight. The base station constructs the feedback weight by filtering the feedback bits over two slots using a sliding window. The resulted phase constellation has four states. Since all consecutive feedback weights use one common feedback bit, the next transmit weight either remains unchanged from the previous or jumps to the neighboring state, as shown in Fig. 19.

Feedback weight verification

As mentioned earlier, the sent feedback bits are prone to errors when transmitted through the uplink channel. This is due to the fact that the bits are sent uncoded

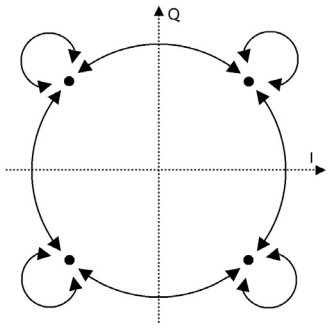

FIGURE 19 Phase constellation in TxAA [Hot03].

to the base station in order to reduce feedback delay and uplink signaling capacity. In case of feedback error, the used weight w_2 is different from the weight signaled by the UE. This imposes performance degradation in two ways. First, the signal combining gain is reduced since the used weight and thus the phase of the sent signal from antenna 2 is not the optimal calculated by the UE. Second, the common channel estimates h_1 and h_2 cannot be reliably combined to obtain a reliable estimate for the dedicated channel.

There are several weight verification formulations which are used to solve the mentioned problem. One option is to compare the dedicated and common channel estimates. This was presented in [Hot03]. In the CL Mode 1 studies presented in this thesis, uplink signaling errors and weight verification are not considered.

Channel model and SINR calculation with single stream TxAA

Using TxAA only one signal is transmitted but it is sent through two paths with different beamforming weights. Thus in order to calculate the SINR the beamformed channel matrix $\mathbf{H}_{BF}$ must be defined:

$$\mathbf{H}_{BF} = \sum_{j=1}^{N_{Tx}} w_j \mathbf{H}_j \,, \tag{39}$$

where w_j is the Tx-weight and $\mathbf{H}_j$ is the channel matrix of Tx-antenna j.

Assuming that TxAA is used for HS-DSCH and for the associated DCH and other channels are transmitted using STTD, the transmit powers can be marked as:

$$\begin{aligned} P_{BF} &= P_{HS\text{-}DSCH} + P_{DCH} \,, \\ P_{omni} &= P_{tot} - P_{BF} \,. \end{aligned} \tag{40}$$

Then SINR for HS-DSCH in the UE receiver for TxAA is calculated as:

$$SINR = \frac{S_f P_{HS\text{-}DSCH} |\mathbf{w}^T \mathbf{H}_{BF}^T \delta_D|^2}{\underbrace{P_{BF} |\mathbf{w}^T \mathbf{H}_{BF}^T \hat{\delta}_D|^2}_{I_{intra}} + I_{omni} + \underbrace{\mathbf{w}^T \mathbf{C}_w \mathbf{w}^*}_{I_{inter}}}, \tag{41}$$

where receiver filters for both Rake and LMMSE equalizer are defined otherwise similarly as in chapter 3 but the beamformed channel matrix is used in the filter coefficient calculation. Multipath interference from the non-beamformed channels (omni-interference) is defined as

$$I_{omni} = \frac{1}{2} \cdot P_{omni} \mathbf{w}^T \left(\sum_{n=1}^{N_{Tx}} \mathbf{H}_n^T \hat{\delta}_D \hat{\delta}_D^T \mathbf{H}_n^* \right) \mathbf{w}^* . \tag{42}$$

Explicit modeling of inter-cell interference

I_{inter} in Eq. 41 presents the inter-cell interference contribution. Note that the impact of set/changed Tx-weights in the neighboring sectors can be modeled explicitly.

Taking into account that TxAA is used also in the neighboring sectors, the total downlink interference from sector i can be divided into beamformed and non-beamformed interference. The total power $P_{tot,i}$ from sector i excluding common pilot power is assumed to be weighted according to the current HSDPA user in sector i and only common pilot power is assumed to cause non-beamformed interference. Thus beamformed interference from sector i is given as

$$I_{i,j}^{BF} = \frac{1}{2} (P_{tot,i} - P_{pilot}) L_i \sum_{l=1}^{N_i} \left(g_{i,l} \left(\| w_{1,i} h_{1,i,l}^j + w_{2,i} h_{2,i,l}^j \|^2 \right) \right), \tag{43}$$

where $P_{tot,i}$ is the total downlink transmission power and P_{pilot} is common pilot power in sector i and L_i is the slow faded path loss between the terminal and sector i. N_i is the number of multipath components provided by the simulated environment without diversity in sector i, $g_{i,l}$ is the average path gain of the l^{th} component, $h_{1,i,l}^j$ and $h_{2,i,l}^j$ are the complex channel coefficients for two Tx antennas of sector i, receive antenna j and multipath component l. $w_{1,i}$ and $w_{2,i}$ are transmit weights for antennas 1 and 2 in sector i for the scheduled HSDPA user. n_0 is thermal noise.

Interference from common pilot channel is given as

$$I_{i,j}^{omni} = \frac{1}{2} P_{pilot} L_i \sum_{l=1}^{N_i} \left(g_{i,l} \left(\| h_{1,i,l}^j \|^2 + \| h_{2,i,l}^j \|^2 \right) \right). \tag{44}$$

This leads to total downlink interference from all the sectors as

$$I_{tot}^j = \sum_{i=1}^{k} \left(I_{i,j}^{omni} + I_{i,j}^{BF} \right) + n_0 . \tag{45}$$

4.2.4 Dual stream TxAA

In 3GPP Release 7 the peak data rate of HSDPA increased by introducing the support for MIMO usage with HS-DSCH. 3GPP extended the TxAA transmit diversity scheme of Release 99 WCDMA to a full MIMO approach including spatial multiplexing. The approach is called D-TxAA. With D-TxAA up to two data streams (transport blocks) can be transmitted simultaneously over the radio channel using the same channelization codes. Each transport block is processed and channel coded separately. After spreading and scrambling, the transmitted streams are precoded based on weight factors to optimize the signal for transmission over the radio channel.

Generally in D-TxAA the UE data in the transmission buffer at the Node B can be sent through either one or two independent data streams on the physical layer. The UE measures the channel quality between all Tx antennas and the UE separately. Separate CQIs are sent for single stream mode and both streams for dual stream mode.

As the Node B schedules the UEs a transmission mode (single or dual stream) which maximizes the achievable throughput is selected. The Node B informs the UE of the used transmission format(s) in HS-SCCH. Only a single HS-SCCH transport block is sent. Node B then allocates independent MCSs for the stream(s) according to the reported CQIs.

The base station weighs the transmitted HS-DSCH signal(s) according to the receiver feedback and transmits the used precoding weight(s) in HS-SCCH to the receiver, eliminating the need for antenna verification.

If single stream mode is selected, the D-TxAA falls back to basic TxAA operation. In case of dual stream mode the form of the received signal y_i of stream i at time instant t can be written as

$$y_i[t] = \left(\sum_{j=1}^{N_{Tx}} w_{i+2(j-1)}[t] h_j[t] \right) x_i[t] + n_i[t] \,, \tag{46}$$

where $h_j[t]$ is the channel impact between the receiver and transmit antenna j at time instant t. It should be noted that the noise $n_i[t]$ includes the interference of the parallel stream. Precoding weight w_k is selected so that

$$\begin{aligned} w_1 = w_3 &= 1/\sqrt{(2)} \,, \\ w_4 &= -w_2 \,, \\ w_2 &= \left[\tfrac{1+j}{2}, \tfrac{1-j}{2}, \tfrac{-1+j}{2}, \tfrac{-1-j}{2} \right] . \end{aligned} \tag{47}$$

Fig. 20 presents the generic structure of D-TxAA transmitter. The receiver is practically the same as with single stream TxAA, shown in Fig. 18. The receiver only calculates and reports the optimal weight w_2.

Fig. 21 presents the achievable throughput of each MCS in single and dual stream mode. All single stream transmissions are allocated a single stream MCS. If scheduler decides to use dual stream transmission for a UE, dual stream MCSs are allocated for both streams according to their individual reported CQIs. Hence

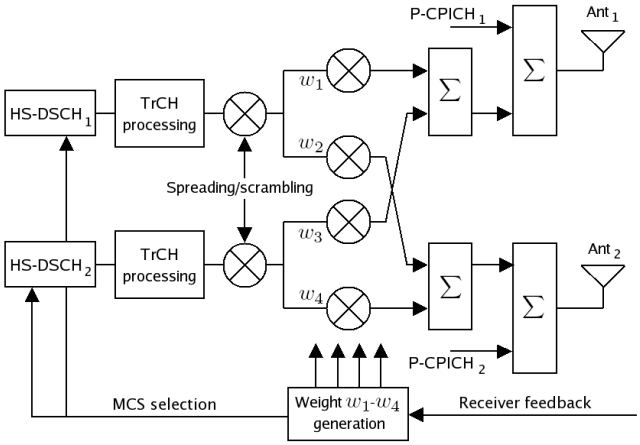

FIGURE 20 The generic downlink transmitter structure to support MIMO operation for HS-DSCH transmission.

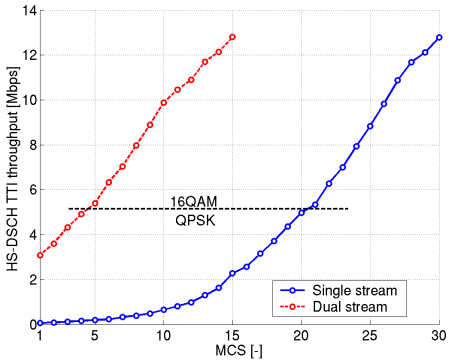

FIGURE 21 Achievable HS-DSCH throughput with single and dual stream MCSs. Used modulation indicated.

if both streams are allocated the highest dual stream MCS, the achievable bit rate is doubled compared to single stream.

Channel model and SINR calculation with dual stream TxAA

In MIMO transmission the receiver consists of two LMMSE equalizer filters, $\mathbf{w}_1$ and $\mathbf{w}_2$, for the primary and for the secondary data stream, respectively. LMMSE solution [Kra00a, Kra00b] leads to equalizer coefficients

$$[\mathbf{w}_1 \ \mathbf{w}_2] = \mathbf{C}_w^{-1}\mathbf{H}_{BF}^H(P_{tot}\mathbf{H}_{BF}\mathbf{C}_w^{-1}\mathbf{H}_{BF}^H + \mathbf{I})^{-1}\delta_D\,. \tag{48}$$

The definition of the coefficients is done similarly as in chapter 3. The combined beamformed channel matrix of both transmit antennas $\mathbf{H}_{BF}$ is defined by

$$\mathbf{H}_{BF} = \begin{bmatrix} \mathbf{H}_{BF,1} \\ \mathbf{H}_{BF,2} \end{bmatrix}, \tag{49}$$

where $\mathbf{H}_{BF,i}$ is the beamformed channel matrix of stream i defined by

$$\mathbf{H}_{BF,i} = \sum_{j=1}^{N_{Tx}} w_{i+2(j-1)} \mathbf{H}_j, \tag{50}$$

where $\mathbf{H}_j$ is the channel matrix between antenna j and the receiver and w_k is one the precoding weights.

SINR calculation is done separately in single and dual stream modes. In dual stream mode the interference of the other stream must be taken into account. SINR for primary stream, assuming only HS-DSCH power is transmitted through the beam, non-beamformed power $P_{omni} = P_{tot} - P_{HS\text{-}DSCH}$ is divided evenly between the transmit antennas and only the primary stream is active, is calculated otherwise similarly as in TxAA case (Eq. 41) but now the beamformed power consists only of HS-DSCH power.

Assuming both streams are active, the code-wise SINR for primary stream becomes

$$SINR_1 = \frac{\frac{S_f}{N_c} P_{BF} \cdot |\mathbf{w}_1^T \mathbf{H}_{BF,1}^T \delta_{D(1)}|^2}{\left(\begin{array}{l} P_{BF} \cdot |\mathbf{w}_1^T \mathbf{H}_{BF,1}^T \hat{\delta}_{D(1)}|^2 + I_{omni} + 2 \cdot \mathbf{w_1}^T \mathbf{C}_w \mathbf{w_1}^* + \\ \underbrace{\frac{S_f}{N_c} P_{BF} \cdot |\mathbf{w}_1^T \mathbf{H}_{BF,2}^T \delta_{D(1)}|^2}_{I_{other}} + \underbrace{P_{BF} \cdot |\mathbf{w}_1^T \mathbf{H}_{BF,2}^T \hat{\delta}_{D(1)}|^2}_{I_{other}^{multipath}} \end{array} \right)}, \tag{51}$$

where N_c is the number of codes, I_{other} is the interference from the other stream after despreading and $I_{other}^{multipath}$ is the multipath interference from the other stream. The non-beamformed interference I_{omni} is defined as in Eq. 42. $SINR_2$ for secondary stream is calculated correspondingly.

5 ACHIEVED RESULTS

In this chapter the used research method and the research scenario are introduced firstly in chapters 5.1 and 5.2, respectively. The achieved results are analyzed in chapter 5.3.

5.1 Research tool

The performance evaluation of different receiver schemes along with receive and transmit antenna diversity is done by means of extensive system simulations using a fully dynamic WCDMA system simulator. The simulator is previously presented in [Häm03]. It is a comprehensive dynamic WCDMA network simulation tool, which is comprised of a detailed model of the physical layer, radio resource management (RRM) and part of the upper layers of a WCDMA radio access network. Also detailed HSDPA and advanced receiver functionality has been added later to this system simulator [Kur05].

The conducted simulations are divided into separate link and system level parts in order to minimize the complexity of the simulator and the simulation time. In the link level simulations the modeling of the transmission between the Node B and a single terminal is done in a very detailed manner. The resulting data is used in the system simulations through a so called actual value interface (AVI). The AVI principle has been previously presented in [Häm97].

The overall simulator flow is as follows.

1. Initialization. All static objects are created (simulation scenario, RNCs and Node Bs).

2. Warm up. Some amount of calls are generated to achieve an initial load in the network.

3. Simulation runs. Calls are being created according to a homogeneous Poisson process. Power levels, interference and signal to noise ratios are calcu-

lated every slot. Statistics are saved slot wise or more sparsely depending on the parameters.

4. Finish. Last statistics are saved and all objects are destroyed.

5.2 Simulation scenario

Two kinds of simulation scenarios were used in the studies. A wrap-around macro cell scenario and a combined macro-femto cell scenario.

5.2.1 Wrap-around macro scenario

First of the simulated HSDPA network in articles **PI-PVII** and **PX** is presented in Fig. 22. It consists of 7 base station sites with 3 sectors each resulting in a layout of 21 hexagonal cells which are numbered in the figure. In this thesis a cell refers to the service area of one sector. The scenario a so called wrap-around scenario, where the UE mobility is limited around the center cells, but the cell transmissions are replicated outside the mobility area to offer more realistic interference situation for every UE in the network. A UE is able to make a handover to the outer cells but if it moves outside the mobility area, its position is moved to the opposite side of the mobility area. The wrap-around simulation methodology has been more thoroughly discussed in [Hyt01].

The inter-site distance is 2800 meters and the theoretical cell border is calculated as the farthest point of the cell from its base station site. The cell radius is 933 meters. Propagation model is a modified Okumura-Hata model presented in [3G01]. It is defined by

$$L[\text{dB}] = 128.1 + 37.6 \log 10(R[\text{km}]). \tag{52}$$

Log-normally distributed slow fading has a 8 dB standard deviation and a spatial correlation distance of 50 meters. Used channel profiles are modified Pedestrian A and Vehicular A. The power delay profiles are modified from the original ITU power delay profiles so that the delay between paths equals at least one chip-time. Average path powers in Pedestrian A channel are in decibels [-0.2, -13.5] and in Vehicular A channel [-3.1, -5.0, -10.4, -13.4, -13.9, -20.4]. The delays of the channel profiles are [0, 1] slots for PedA and [0, 1, 3, 4, 7, 10] slots for VehA. MAC-hs packet scheduling is based on round robin and proportional fair scheduling algorithms without code-multiplexing, i.e. only one UE is scheduled per TTI. The maximum numbers of HS-DSCH codes are 5 and 10 with spreading factor 16. HS-DSCH power is 14 W, which is 70 % of the total base station transmission power. One code is allocated for HS-SCCH with spreading factor of 128 and HS-SCCH is ideally decoded. HS-DSCH link adaptation is based on the UE reported channel quality indicators (CQIs) (inner loop) and UE reported ACK/NACKs from past retransmissions (outer loop). CQI measurement error

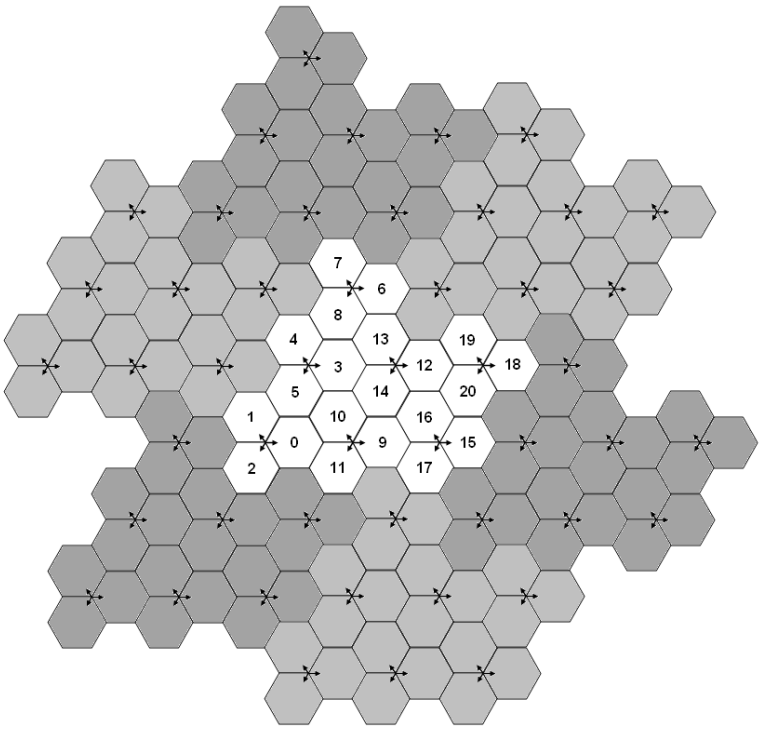

FIGURE 22 Simulation scenario.

standard deviation is 1 dB. Aimed block error rate (BLER) target for the first transmission is 30 % and outer loop link adaptation is used to control the BLER target. CQI tables are throughput optimized with BLER target of 30 %. Six parallel stop-and-wait (SAW) channels are used for the Hybrid ARQ and maximum of 4 retransmissions are allowed per transport block. Chase Combining is used for the retransmissions [Cha85].

Signaling of CQI on the uplink HS-DPCCH is modeled with a fixed delay of 1 TTI and with ideal decoding. Probabilities of erroneous acknowledgement interpretations are 0.01 (ACK as NACK or DTX as ACK) and 0.001 (NACK as ACK). DTX as ACK (discontinuous transmission) means that no acknowledgement is sent due to erroneous reception of HS-SCCH but the transmitter interprets this as an acknowledgement.

Mobility and traffic models are based on [3G98] and default UE velocity is 3 km/h. Traffic model is a modified web browsing model in which the users do not have a reading time during a download session i.e. they only have one packet call per session. Simulation time is 6 minutes. The call arrival rate in the network is 140 calls per second and the packet call size determined by

$$PacketSize = min(P, m)\,, \tag{53}$$

where P is normal Pareto distributed random variable (α=1.1, k=21500 bytes) and m=5000000 bytes, which is the maximum allowed packet size. Using these parameters the average packet call size is 112 kilobytes. Thus, the total average offered load per cell can be calculated as $A * B/C$, where A is the call arrival rate, B is the average packet call size and C is the number of cells in the network. In the simulations the average offered load per cell is approximately 6 Mbps. New calls are generated according to homogeneous Poisson process and the offered traffic is high enough to have almost 100 % utilization of the HS-DSCH. Admission control allows up to 16 HSDPA users per cell.

5.2.2 Combined macro-femto cell scenario

A combined macro and indoor scenario was used in articles **PVIII**-**PIX**. The scenario layout is presented in Fig. 23. 18 macro base transceiver stations (BTSs) are situated with inter-site distance of 2800 meters. On top of 6 central cells there is a mobility area of approximately 6.9 km^2 where the users move. In the mobility area there are 37 buildings having uniform separation to their neighboring buildings. Building layout and a mobility area surrounding it is depicted in Fig. 24. The area of a single building is 300 m^2. Each building is equipped with a femto BTS, which is situated at the center of the building. Building walls do not restrict users' mobility but they do affect the signal propagation.

In the simulations two kinds of users are created in the network: macro users and dedicated indoor users. Macro users are created randomly around the mobility area and their mobility is restricted only inside it. They can enter and exit the buildings and their mobility areas. Indoor users are created randomly to building mobility areas and their mobility is limited inside the area in which they are created. It should be noted that UEs that are created in the building mobility area are referred as indoor UEs in this paper, although they may also be outdoors inside the building mobility area.

A user is allowed to connect to any of the femto BTSs and the 6 central macro BTSs and is allowed to make handover from one to another. However, as femto cells are intended to be used by a dedicated group of users only, access restriction of unauthorized users to femto cells were modeled by limiting the maximum HSDPA queue length to 3 users. The surrounding 12 macro BTSs are interferers, i.e. they only create HSDPA transmission-like interference and a UE cannot establish a connection or make a handover to them. The macro and femto BTS parameters are presented in Table 6. The packet call size is calculated similarly as in Eq. 53 but now k=50000 bytes, resulting in average packet call size of 2345 kilobytes, as shown in Table 6.

Signal propagation and channel model

Macro propagation is the same as presented in Eq. 52. Indoor propagation is modeled with a modified COST 231 multi-wall model [Dam98] without the effect of floor attenuation (since the buildings have only one floor) defined by

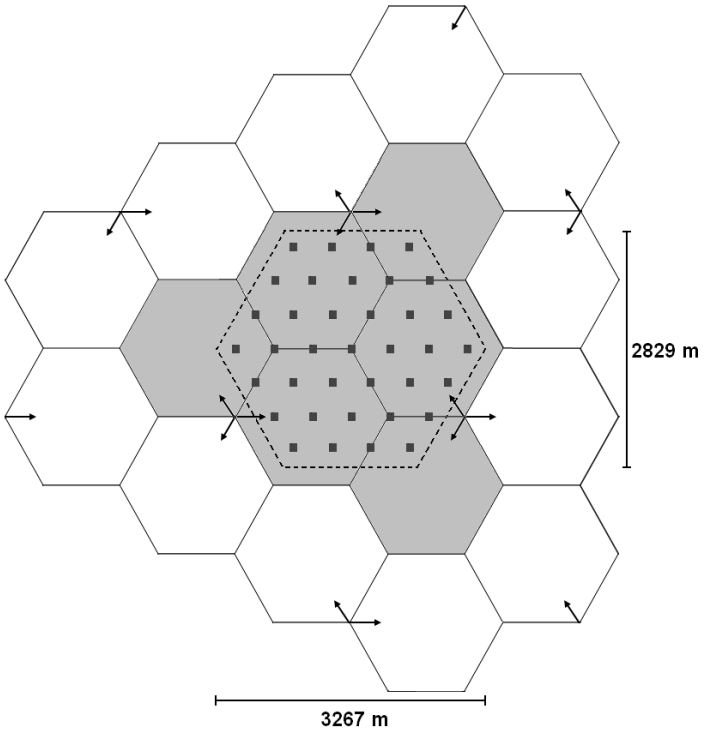

FIGURE 23 Combined macro and indoor scenario. Building grid and macro mobility area (dashed line) depicted at the center.

$$L[\text{dB}] = 37 + 3.2 \cdot 10 \log_{10}(R[\text{m}]) + L_w n_w, \tag{54}$$

where 37 dB constant is the path loss at reference distance 1 m, R is the distance between the transmitter and the receiver in meters, n_w is the number of indoor walls between them and L_w is the attenuation of an indoor wall. Used wall attenuation parameters along with other main simulation parameters different from wrap-around macro scenario are presented in Table 7.

In the scenario there are different situations where the UE and the BTS can be located in relation to each other. The signal propagation must be calculated individually in each of them:

- *BTS and UE both outdoors:* Macro model
- *Other outdoors, other indoors:* Macro model + external wall loss
- *Both indoors and in the same building:* Indoor model
- *Both indoors but in different buildings:* Macro model + 2 $\times$ external wall loss

Also the used channel model is twofold, as the UE and BTS locations are considered: if both UE and BTS are in the same building, ITU Pedestrian A channel

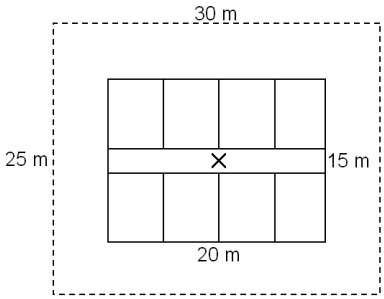

FIGURE 24 Building layout and building mobility area (dashed line). Femto BTS location depicted in the center.

TABLE 6 BTS parameters.

	Macro BTS	Femto BTS
No of BTSs	6 serving, 12 interfering	37
Site separation	2800 m	467 m
Antenna type	3-sector	omni-directional
Max Tx power	43 dBm	15 dBm
Pilot power	33 dBm	4 dBm
HS-DSCH power	70 % of total BTS Tx power	
HS-SCCH power	Power controlled. Max. 10 % of total BTS Tx power	
Max. HSDPA queue length	16	3
Interferer Tx power	41.5 dBm	-
Interferer average activity	80 %	-

model is used. Otherwise, the model is Vehicular A. In the sake of modeling simplicity both channel model power delay profiles are modified so that the delays are integer chips.

5.3 Simulation result analysis

The objective of this thesis is firstly to analyze the WCDMA HSDPA network performance when advanced receivers, namely LMMSE chip-level linear equalizers are used in UEs. The analysis also extends to different antenna diversity methods thus studying the effect of using receive diversity at the UE and different transmit diversity techniques at Node B. Dynamic system level simulations are conducted with different advanced receiver penetrations which are compared to the results with a basic single rake receiver. Different fading (UE velocity), multipath propagation conditions (Pedestrian A and Vehicular A channels), radio cell

TABLE 7 Simulation parameters.

Slow fading spatial correlation	5 m
Channel profile	PedA, if UE and BTS in the same building VehA, otherwise
Packet scheduler	Proportional fair
Max no. of multicodes	15
Building outer wall loss	15 dB
Building inner wall loss	3 dB
Traffic model	Modified web browsing (no reading time)
Average packet call size	2345 KB
Network offered load	12.506 Mbps per macro BTS

sizes (macro and femto cells) as well as a basic and an advanced scheduling algorithm (round robin and proportional fair, respectively) were also taken into account thus covering various realistic network conditions.

5.3.1 Receive diversity and LMMSE chip-equalizer

Receive diversity and LMMSE chip level equalization performance in HSDPA network has been presented in the included articles **PI** and **PV**. The UE receive diversity and equalizer can be considered as complementing features as they both improve system performance. The schemes provide gain through two different means: the equalizer provides higher bit rates near the cell center where the intra-cell interference can be canceled, whereas receive diversity improves the throughput at cell border where additional signal energy is required in the fight against inter-cell interference.

UE velocity impact was seen mainly from going from 3 to 30 km/h. Increasing the velocity even more had only a little impact on throughput. This indicates that the gain of link adaptation is mainly lost already at lower velocities. However, as the influence of velocity was quite similar on every receiver, the gain of advanced receivers was seen to be rather constant throughout the whole range of simulated velocities.

The simulations with different advanced receiver penetrations were presented in the included articles **PII** and **PV**. The results indicated that even a small portion of advanced receivers in the network subscribers increase the average cell and user throughput. It was also observed that having advanced receivers in the network increases not only the overall throughput but also the throughput of conventional rake 1×1 users. This can be explained by the phenomenon that users who are close to serving sector will experience higher bit rates, thus their calls will be shorter leading to more frequent scheduling of distant users.

Receive diversity seems to be the most prominent of the advanced receiver

schemes. Dual antenna receiver with chip-equalization offers the best performance in all cases. As the impact of different parameters was evaluated, the amount of superiority of the dual antenna receiver with conventional rake over the conventional single antenna chip-equalizer depends on the selected setting.

5.3.2 Advanced scheduling

Advanced scheduling algorithm, namely proportional fair, performance was compared to basic round robin scheduling in articles **PI** and **PV**.

It was found that PF has the best performance in Pedestrian A channel as higher SINR deviation result to higher gains. This is due to PF accounting individual users' channel conditions in scheduling. Thus the highest benefit from PF was achievable when channel variations are high, but not too fast to be able to be traced with CQI reporting messages. Gain from PF scheduler dropped quite clearly from 3 to 30 km/h, especially with 1×1 receivers but with receiver diversity schemes PF scheduler was able to give small gain up to 120 km/h UE velocity.

5.3.3 STTD and single stream TxAA performance

HSDPA network performance with single stream transmit diversity schemes along with advanced receivers and receive diversity was studied in the included article **PIII**. The performance of STTD was seen to be worse in terms of cell throughput compared to 1-Tx cases in all the simulated scenarios. The loss is only minor with rake receivers, but with equalizer STTD leads to quite a high loss in terms of cell throughput. As STTD reduces SINR variance the loss in cell throughput with PF scheduler is as expected.

It was observed that using TxAA a clear gain is achieved with both schedulers compared to 1-Tx cases with both conventional rake and also with LMMSE equalizer receiver, especially when using only a single receive antenna. Using receive diversity along with TxAA was also beneficial but the gains were lower compared to 1-Rx. This was due to the fact that Tx diversity gives less coverage gain on top of Rx diversity. With RR TxAA provides good gains for other receivers than 2-Rx equalizer. It does not change the performance order of different receivers with 1-Tx, but it reduces the gains from 2-Rx as compared to 1-Rx. With PF scheduler TxAA provides rather good gains with all receiver schemes as compared to 1-Tx. Most notable is that TxAA with 1-Rx equalizer provides better cell throughput than 2-Rx rake and almost the same throughput as 2-Rx rake with TxAA. It could be said that TxAA provides a good evolutionary path with 1-Rx equalizers.

The performance of HSDPA network with closed loop transmit diversity with reduced inter-cell interference predictability was studied in the included article **PIV**. The results correspond well to earlier findings e.g. presented in [Ber04] in that it can be concluded that WCDMA/HSDPA system is robust enough to handle the small additional SINR fluctuations which could be caused by e.g.

closed loop transmit diversity operation. Link adaptation outer loop compensates the variation that is caused by the Tx-weight adaptation in neighboring sectors and ensures that retransmission probabilities stay at the desired level.

Thanks to efficient HARQ operation and inherent radio channel quality report errors of the system no indication of the problems claimed in [Rin05] and [Oss05] were seen even with these fully dynamic system simulations, where interference was explicitly modeled, and which are thereby considered to reflect reality rather well.

5.3.4 MIMO performance with HSDPA

The comparison of 1x2 receive diversity to 2x2 closed-loop MIMO schema in HSDPA system was done in article **PX**. According to the results, studied 2x2 MIMO schemes can give significant gain over traditional receive diversity when spatial multiplexing can be effectively used. High SINR values and up-to-date link adaptation feedback are essential requirements for this. According to the conducted studies, the performance gain of 2x2 MIMO over 1x2 is about 12-15 % in the studied environment considering the physical layer improvement. The gain of MIMO from the user perspective depends on the offered load in the network. High load increases the queuing times and thus diminishes the impact of physical layer bit rate to the call bit rate. In this sense the impact of MIMO can be even less from the user point of view. Although users near the base station can achieve up to 30 % call bit rate gain despite the high offered load, the relatively low gains in physical layer bit rate and in the call bit rates in average indicate that micro or pico cell environment is needed to fully realize the gains promised by MIMO theory.

5.3.5 Inter-cell interference cancellation

In article **PVI** the performance benefit of interference aware LMMSE chip level equalizers with and without receiver diversity was evaluated. The results indicated that the gains of interference aware LMMSE equalizer receiver were the highest at the cell border regions where high DIR values were realized, especially with receive diversity. With single receive antenna very low gains were observed even at the cell borders.

In terms of user throughput, using interference aware equalizer with receive diversity seemed to provide benefits by increasing the cell border throughputs by slightly over 20 %. For the instantaneous HS-DSCH TTI throughput the observed gains were smaller, lying in the range of 15 %. Thus it seemed that the evaluated receivers would be able to provide benefits for the end user experience by increasing the achievable data rates at the cell edges, but having a minor effect to the average system performance.

A more general approach in the evaluation of inter-cell interference cancellation performance in system point of view was taken in article **PVII** where different ideal inter-cell interference cancellation efficiencies with and without receive diversity and advanced receivers was evaluated.

The observed gain of inter-cell interference reduction was the highest with equalizer receivers. This was as expected since with rake the intra-cell interference dominates. The number of receive antennas did not affect the achievable gains, i.e. the difference between single and dual antenna receivers remained the same throughout simulated interference reduction efficiencies.

It could be concluded that inter-cell interference cancellation is beneficial only if it can be done very efficiently. It was noticed that the portion of users that suffer from inter-cell interference is relatively small. Thus, with low cancellation efficiencies, i.e. 20 % or lower, the benefit in cell and user throughput is nominal. When the interference reduction efficiency is increased, the benefit is first visible in user throughput and then in system throughput. Only with inter-cell interference cancellation percentages of 30 % or higher the benefit is considerable with both metrics.

5.3.6 Femto cell performance

The performance of HSDPA network with and without the use of low transmission power (femto) BTSs using the same carrier as the underlaying macro cell network was presented in article **PVIII**. Co-channel femto cells were noticed to have a significant impact on the HSDPA performance especially in a fully loaded network. 15-20 % gain in network throughput was seen with a full network load despite the relatively long distance in average between femto BTS and its users. Due to users being uniformly distributed in the network, the gain comes mainly from the fact that the load is distributed between higher number of access points. Using femto BTSs decreased the average number of users in HSDPA queue by 10-20 % with the highest load, which in part increased average user throughputs by 33-65 %, depending on the receiver scheme.

The femto BTSs are intended to a home or an office building use where there are constantly users near the base station. However, it was seen that femto BTSs are able to offer significant gains in an HSDPA network especially from the user point of view even when the users of the femto BTSs are not concentrated near the BTSs.

The performance of an HSDPA network consisting of femto cells on top of an underlying macro cell network with and without the use of a higher order modulation, namely 64QAM, in addition to QPSK and 16QAM was evaluated in article **PIX**. Also the effect of different indoor UE penetrations was studied. Increasing indoor UE penetration was seen to increase user and network bit rates considerably when femto BTSs were employed. The gain over a scenario where macro cells provided the whole network coverage was seen to be in the range of hundreds of percents in terms of both system and user throughput.

Due to intra-cell interference limited SINR, rake receiver was not seen to benefit from 64QAM, even with receive diversity. Rake users practically never realized high enough SINRs to use 64QAM MCSs. Only the equalizer was seen to benefit from 64QAM, especially with Rx diversity. The gain was visible mainly in user throughputs with even a small amount of dedicated indoor users.

6 CONCLUSIONS

In this thesis the system level performance of several performance enhancing features of High Speed Data Packet Access (HSDPA) concept of Wideband Code Division Multiple Access (WCDMA) technique were studied. The analysis considered the performance of a conventional rake reception algorithm and an advanced signal reception algorithm, Linear Minimum Mean Squared Error chip level equalizer (LMMSE).

It was found that the equalizer provides higher bit rates near the cell center where the intra-cell interference can be canceled. The gain was visible with all code resource and scheduler combinations. If a conventional rake receiver with a proportional fair scheduler is used as a reference, the gain of mere equalization in a macro cell scenario was around 30-50 % in cell throughput. However, the benefit of equalizer is heavily dependent on the users locations in the serving cell. Thus, the result of the comparison between equalizer and receive diversity is dependent on the selected parameters. Using receive diversity instead was seen to offer 50-100 % gain in the same scenario, depending on the parameters. Employing both techniques a gain in the range of 120-180 % is achieved.

It was also seen that even a small portion of advanced receivers in the network subscribers increased the average cell and user throughput. Having advanced receivers in the network increased not only the overall throughput but also the throughput of conventional rake 1×1 users.

An advanced scheduling algorithm, namely proportional fair, was mainly seen to improve 1-Rx receiver throughputs. The gain in cell throughput was in the range of 60 % with 1×1 and 25 % with 1×2 cases. In Pedestrian A channel the gains were higher due to PF being able to exploit the high SINR variance of the channel.

Open loop scheme Space-Time Transmit Diversity (STTD) performance was negative with all simulated scenarios, especially with proportional fair scheduler. This was as expected since STTD decreases channel variations which are crucial to the good performance of PF.

Single stream closed loop transmit diversity scheme Transmit Antenna Array (TxAA) improved 1-Rx antenna receiver throughput by approximately 25 %

but offered a mere 5 % increase to cell throughput with UEs already employing receive diversity.

Full MIMO approach dual stream TxAA was not seen to significantly improve the performance of single stream TxAA in a macro cell scenario. The gain over 1×2 equalizer was in the range of 15 %. It was concluded that more isolated cell structures are needed to achieve higher gains from MIMO.

Employing several low transmit power femto cells in a macro cell network offered around 15 % gains with all receiver and receive antenna scheme combinations compared to a plain macro cell base station scenario. The users uniform locations in the macro cell scenario resulted in the gain coming mainly from the the network load being distributed to a higher amount of access points. Thus, the gains were the same despite the used receiver scheme.

Increasing the user density near the femto cells resulted in huge gains in cell and user throughputs with all receivers. The gain of LMMSE equalization over rake reception increased also. With all users being near the femto cells the gain of mere equalization was in the range of 100 % and the gain of 1×2 and equalizer over 1×1 rake was around 220 %. At the same time receive diversity alone improved cell throughput by approximately 50 %.

In low signal energy regions the intra-cell interference mitigating LMMSE equalizer was not seen to offer any gain. At the cell border its performance degraded to rake level. Assuming knowledge of the inter-cell interference, i.e. neighboring base station transmissions, improved the equalizer performance by 5-10 % in overall but the highest performance was seen by the UEs at the cell borders achieving as high as 20 % gain from the interference aware equalization.

In general, inter-cell interference cancellation was seen to be beneficial only if it can be done very efficiently. It was noticed that the portion of users that suffered from inter-cell interference was relatively small. Thus, with low cancellation efficiencies, i.e. 20 % or lower, the benefit in cell and user throughput was nominal.

YHTEENVETO (FINNISH SUMMARY)

Wideband Code Division Multiplexing (WCDMA) -tekniikka on laajimmin käyttöön otettu kolmannen sukupolven (3G) matkaviestinverkkojen ilmatien rajapintatekniikka maailmassa. 3G-liikenteen kasvu ja uusien sovellusten bittinopeusvaatimusten kasvava tarve vaatii 3G-verkkojen ilmarajapintatekniikan jatkuvaa kehitystyötä.

Tässä väitöskirjassa tutkitaan useiden WCDMA-tekniikan kehittyneiden lähetin- ja vastaanotinalgoritmien suorituskykyä yksin ja yhdessä toistensa kanssa. Pääasiassa tutkimus käsittää suorituskykyvertailun perinteisen rake-vastaanottimen ja kehittyneen Linear Minimum Mean Squared Error (LMMSE) -taajuuskorjainvastaanottimen välillä, kun käytössä on WCDMA:n High Speed Downlink Packet Access (HSDPA) -tekniikka, joka mahdollistaa erittäin korkeat datanopeudet WCDMA:n laskevalla siirtotiellä.

Vastaanottimien toimintaa on tarkasteltu erilaisten antennidiversiteettitekniikoiden kanssa sekä vaihtelemalla useita HSDPA-verkon parametreja. Parametreina ovat muun muassa kanavaprofiili, HSDPA:lla käytössä olevien rinnakkaisten koodikanavien määrä, verkon solukoko, kehittyneiden vastaanottimien osuus verkon käyttäjistä, käyttäjien nopeus sekä vastaanottimen kyky vähentää naapurisolujen aiheuttamaa häiriötä. Lisäksi erilaisten HSDPA-lähetysvuoron jakoalgoritmien suorituskykyä on vertailtu.

Lähetindiversiteettitekniikoista on keskitytty avoimen silmukan konsepteista Space-Time Transmit Diversity (STTD) -tekniikkaan ja suljetun silmukan konsepteista Transmit Antenna Array (TxAA) -tekniikkaan, josta tutkimuksen kohteena ovat yhden ja kahden datavuon tekniikat. Lisäksi on tutkittu naapurisolun häiriön vaikutusta yhden datavuon TxAA:n suorituskykyyn.

Tutkimusmenetelmänä ovat olleet kattavat systeemisimulaatiot käyttäen työkaluna dynaamista WCDMA-verkkosimulaattoria, joka sisältää tarkat mallinnukset signaalin etenemismalleista, käyttäjien liikkuvuudesta, liikennemalleista, radioresurssien hallinta-algoritmeista sekä WCDMA-radioverkon fyysisestä kerroksesta että osasta ylemmistä protokollakerroksista.

REFERENCES

[3G98] 3GPP, Selection procedures for the choice of radio transmission technologies of the UMTS, *Technical Report TR 30.03U (V3.2.0)*, March 1998.

[3G01] 3GPP, Physical layer aspects of UTRA High Speed Downlink Packet Access (Release 4), *Technical Specification TS 25.848 (V4.0.0)*, Technical Specification Group Radio Access Network, March 2001.

[3G04a] 3GPP Technical Specification Group Radio Access Network, Physical layer procedures (FDD), *Technical Specification TS 25.214 (V6.2.0)*, July 2004.

[3G04b] 3GPP Technical Specification Group Services and System Aspects, General Universal Mobile Telecommunications System (UMTS) architecture (Release 6), *Technical Specification TS 23.101 (V6.0.0)*, December 2004.

[3G05] 3GPP Technical Specification Group Radio Access Network, Physical channels and mapping of transport channels onto physical channels (FDD) (Release 5), *Technical Specification TS 25.211 (V5.7.0)*, December 2005.

[3G06b] 3GPP Technical Specification Group Radio Access Network, UTRAN overall description (Release 7), *Technical Specification TS 25.401 (V7.2.0)*, December 2006.

[3G06c] 3GPP Technical Specification Group Radio Access Network, High Speed Downlink Packet Access (HSDPA), Overall description, Stage 2 (Release 7), *Technical Specification TS 25.308 (V7.0.0)*, March 2006.

[3G07a] 3GPP home page, *http://www.3gpp.org/*, November 2007.

[3G07b] 3GPP Technical Specification Group Radio Access Network, Physical layer - General description, *Technical Specification TS 25.201 (V7.2.0)*, March 2007.

[3G07c] 3GPP Technical Specification Group Radio Access Network, Multiple Input Multiple Output in UTRA, *Technical Report TR 25.876 (V7.0.0)*, March 2007.

[Ala98] S. M. Alamouti, A Simple Transmit Diversity Technique for Wireless Communications, *IEEE Journal on Selected Areas in Communications, Vol. 16, no. 8, pp. 1451-1458*, October 1998.

[Ber04] L. T. Berger, P. E. Mogensen, T. E. Kolding, F. Frederiksen, K. I. Pedersen, Effects of other-sector interference variation on detection, link adaptation and scheduling in HSDPA, *Proceedings of the Nordic Radio Symposium, Oulu, Finland*, August 2004.

[Cha85] D. Chase, Code combining - A maximum likelihood decoding approach for combining an arbitrary number of noisy packets, *IEEE transactions on communications, Vol. 33, no. 5, pp. 385-393*, May 1985.

[Cla07] H. Claussen, Performance of macro- and co-channel femtocells in a hierarchical cell structure, *Proceedings of the 18th International Symposium on Personal, Indoor and Mobile Radio Communications (PIMRC), Athens, Greece*, September 2007.

[Dam98] E. Damosso (ed.), Digital Mobile Radio Towards Future Generation Systems, *COST 231 final report*, 1998.

[Div98] D. Divsalar, M. K. Simon, D. Raphaeli, Improved parallel interference cancellation for CDMA, *IEEE Transactions on Communications, Vol. 46, no. 2, pp. 258-268*, February 1998.

[Fos98] G. J. Foschini, M. J. Gans, On limits of wireless communications in a fading environment when using multiple antennas, *Wireless Personal Communications, Vol. 6, pp. 311-335*, 1998.

[Fre02] F. Frederiksen, T. E. Kolding, Performance and modeling of WCDMA/HSDPA transmission/H-ARQ schemes, *in IEEE Vehicular Technology Conference (VTC) 2002 Fall, pp. 472-476, Vancouver, Canada*, September 2002.

[Ges03] D. Gesbert, M. Shafi, D. Shiu, P. J. Smith, A Naguib, From theory to practice: An overview of MIMO space-time coded wireless systems, *in IEEE Journal on Selected Areas in Communications, Vol. 21, No. 3, pp. 281-302*, April 2003.

[Gol03] A. Goldsmith, S. Jafar, N. Jindal, S. Vishwanath, Capacity limits of MIMO channels, *IEEE Journal on Selected Areas in Communications, Vol. 21, No. 5, pp. 684-702*, 2003.

[Hai04] V. Haikola, M. Lampinen, T. Saukkonen, HSDPA Performance with parallel interference cancellation, *Proceedings of the 15th International Symposium on Personal, Indoor and Mobile Radio Communications (PIMRC), Vol. 4, pp. 2318-2322, Barcelona, Spain*, September 2004.

[Hei04] M. J. Heikkilä, K. Majonen, Increasing HSDPA throughput by employing space-time equalization, *Proceedings of the 15th International Symposium on Personal, Indoor and Mobile Radio Communications (PIMRC), Barcelona, Spain*, September 2004.

[Hid06] T. Hidekazu, A Hiroyuki, H. Kenichi, S. Mamoru, System-level Evaluations on User Throughput Using MIMO Multiplexing in HSDPA, *Technical report of the Institute of Electronics, Information and Communication Engineers, RCS, Vol. 106, No. 305, pp. 49-53*, 2006.

[Hil05] K. Hiltunen, B. Olin, M. Lundevall, Using dedicated in-building systems to improve HSDPA indoor coverage and capacity, *Proceedings of IEEE Vehicular Technology Conference (VTC) 2005 Spring, pp. 2379-2383, Stockholm, Sweden*, May 2005.

[Ho07] L. T. W. Ho, H. Claussen, Effects of user-deployed, co-channel femtocells on the call drop probability in a residential scenario, *Proceedings of the 18th International Symposium on Personal, Indoor and Mobile Radio Communications (PIMRC), Athens, Greece*, September 2007.

[Hoo02] K. Hooli, M. Juntti, M. J. Heikkilä, P. Komulainen, M. Latva-aho, J. Lilleberg, Chip-Level Channel Equalization in WCDMA Downlink, *EURASIP Journal on Applied Signal Processing, no. 8, pp. 757-770*, 2002.

[Hoo03] K. Hooli, Equalization in WCDMA terminals, Ph.D. thesis, ISBN 951-42-7183-1, University of Oulu, 2003.

[Hol00] J. M. Holtzman, CDMA forward link waterfilling power control, *Proceedings of the 51st IEEE Vehicular Technology Conference, pp. 1636-1667, Tokyo, Japan*, May 2000.

[Hol04] H. Holma, A. Toskala (eds.), WCDMA for UMTS: Radio Access for Third Generation Mobile Communications, Third Edition, John Wiley & Sons Ltd., Chichester, England, 2004.

[Hol06] H. Holma, A. Toskala (eds.), HSDPA/HSUPA for UMTS: High Speed Radio Access for Mobile Communications, John Wiley & Sons Ltd., Chichester, England, 2006.

[Hot03] A. Hottinen, O. Tirkkonen, R. Wichman, Multi-antenna Transceiver Techniques for 3G and Beyond, John Wiley & Sons Ltd., Chichester, England, 2003.

[Hot06] A. Hottinen, M. Kuusela, K. Hugl, J. Zhang, B. Raghothaman, Industrial embrace of smart antennas and MIMO, *IEEE Wireless communications, Vol. 13, No. 4, pp. 8-16*, August 2006.

[Hyt01] T. Hytönen, Optimal wrap-around network simulation, *Helsinki University of Technology Institute of Mathematics Research Reports A432*, 2001.

[Häm03] S. Hämäläinen, WCDMA radio network performance, Ph.D. thesis, ISBN 951-39-1402-X, University of Jyväskylä, 2003.

[Häm97] S. Hämäläinen, P. Slanina, M. Hartman, A. Lappeteläinen, H. Holma, O. Salonaho, A novel interface between link and system level simulations, *Proceedings of ACTS Summit 1997, pp. 599-604, Aalborg, Denmark*, October 1997.

[ITU97] ITU-R, Guidelines for the evaluation of radio transmission technologies for IMT-2000,*Recommendation ITU-R M.1225*,1997.

[Kol02] T. E. Kolding, F. Frederiksen, P. E. Mogensen, Performance Aspects of WCDMA Systems with High Speed Downlink Packet Access (HSDPA), *Proceedings of the IEEE Vehicular Technology Conference (VTC) 2002 Fall, pp. 477-481, Vancouver, Canada*, September 2002.

[Kol03] T. E. Kolding, K. I. Pedersen, J. Wigard, F. Frederiksen, P. E. Mogensen, High Speed Downlink Packet Access: WCDMA Evolution, *IEEE Vehicular Technology Society News*, February 2003.

[Kom00] P. Komulainen, Space-Time Equalization for Interference Suppression in CDMA Terminals, *in Finnish Wireless Communications Workshop (FWCW), Oulu, Finland*, 2000.

[Kov06] I. Z. Kovacs, K. I. Pedersen, J. Wigard, F. Frederiksen, T. E. Kolding, HSDPA performance in mixed outdoor-indoor micro cell scenarios, *Proceedings of the 17th International Symposium on Personal, Indoor and Mobile Radio Communications (PIMRC), Helsinki, Finland*, September 2006.

[Kra00a] T. P. Krauss, M. D. Zoltowski, G. Leus, Simple MMSE equalizers for CDMA downlink to restore chip sequence: Comparison to zero-forcing and Rake, *Proceedings of the IEEE International Conference on Acoustics, Speech, and Signal Processing (ICASSP), pp. 2865-2868, Istanbul, Turkey*, June 2000.

[Kra00b] T. P. Krauss, M. D. Zoltowski, Oversampling diversity versus dual antenna diversity for chip-level equalization on CDMA downlink, *Proceedings of the IEEE Sensor Array and Multichannel Signal Processing Workshop, pp. 47-51, Cambridge, USA*, March 2000.

[Kur05] J. Kurjenniemi, A Study of TD-CDMA and WCDMA Radio Network Enhancements, Ph.D. thesis, ISBN 951-39-2296-0, University of Jyväskylä, 2005.

[Lam05] M. Lampinen, V. Haikola, Open-loop MIMO extensions for HSDPA with practical constraints, *Proceedings of the 16th International Symposium on Personal, Indoor and Mobile Radio Communications (PIMRC), pp. 1688-1692, Berlin, Germany*, September 2005.

[Lat99] M. Latva-Aho, Advanced receivers for wideband CDMA systems, Ph.D. thesis, ISBN 951-42-5039-7, University of Oulu, 1999.

[Lov03] R. Love, K. Stewart, R. Bachu, A. Ghosh, MMSE equalization for UMTS HSDPA, *Proceedings of the IEEE Vehicular Technology Conference (VTC) 2003 Fall, pp. 2416-2420, Orlando, USA*, October 2003.

[Lov04] R. Love, A. Ghosh, W. Xiao, R. Ratasuk, Performance of 3GPP high speed downlink packet access (HSDPA), *Proceedings of the 60th Vehicular Technology Conference (VTC) 2004 Fall, Vol. 5, pp. 3359-3363, Los Angeles, USA*, September 2004.

[Luc03] Lucent Technologies, SINR computation in system simulations with multipath channels and arbitrary linear FIR space-time receivers, *3GPP-3GPP2 spatial channel modelling ad hoc SCM-AHG SCM-105*, January 2003.

[Maj04] K. Majonen, M. J. Heikkilä, Comparison of Multiantenna Technigues for High-Speed Packet Communication, *Proceedings of the 15th International Symposium on Personal, Indoor and Mobile Radio Communications (PIMRC), Barcelona, Spain*, September 2004.

[Nak02] M. Nakamura, Y. Awad, S. Vadgama, Adaptive control of link adaption for high speed downlink packet access (HSDPA) in WCDMA, *Proceedings of the 5th International Symposium on Wireless Personal Multimedia Communications (WPMC), pp. 382-386, Honolulu, Hawaii*, October 2002.

[Oss04] A. Osseiran, A. Logothetis, System performance of transmit diversity methods and a two fixed-beam system in WCDMA, *Wireless Personal Communications, no. 31, pp. 33-50*, 2004.

[Oss05] A. Osseiran, A. Logothetis, Closed loop transmit diversity in WCDMA HS-DSCH, *Proceedings of the IEEE Vehicular Technology Conference (VTC 2005-Spring), Vol. 1, pp. 349-353, Stockholm, Sweden*, May 2005.

[Par01] S. Parkvall, E. Dahlman, P. Frenger, P. Beming, M. Persson, The evolution of WCDMA towards higher speed downlink packet data access, *Proceedings of the IEEE Vehicular Technology Conference (VTC) 2001 Spring, pp. 2287-2291, Rhodes, Greece*, May 2001.

[Ped04] K. I. Pedersen, T. F. Lootsma, M. Stotrupp, F. Frederiksen, T. E. Kolding, P. E. Mogensen, Network Performance of Mixed Traffic on High Speed Downlink Packet Access and Dedicated Channels in WCDMA, *Proceedings of the 60th Vehicular Technology Conference (VTC) 2004 Fall, Vol. 6, pp. 4496-4500, Los Angeles, USA*, September 2004.

[Pol04] A. Pollard, M. J. Heikkilä, A System level evaluation of multiple antenna schemes for high speed downlink packet access, *Proceedings of the 15th International Symposium on Personal, Indoor and Mobile Radio Communications (PIMRC), pp. 1732-1735, Barcelona, Spain*, September 2004.

[Ram02] J. Ramiro-Moreno, K. I. Pedersen, P. E. Mogensen, Radio resource management for WCDMA networks supporting dual antenna terminals, *Proceedings of the IEEE Vehicular Technology Conference (VTC) 2002 Spring, pp. 694-698, Birmingham, USA*, May 2002.

[Ram03] J. Ramiro-Moreno, K. I. Pedersen, P. E. Mogensen, Network performance of transmit and receive antenna diversity in HSDPA under different packet scheduling strategies, *Proceedings of the 57th semiannual IEEE Vehicular Technology Conference (VTC) 2003 Spring, pp. 1454-1458, Jeju, Korea*, April 2003.

[Rin05] M. Ringström, D. Astély, B. Göransson, On closed loop transmit diversity for HSDPA - using an orthogonality matrix for system level evaluations, *Proceedings of the IEEE Vehicular Technology Conference (VTC 2005-Spring), Vol. 1, pp. 344-348, Stockholm, Sweden*, May 2005.

[Rys06] P. Rysavy, Mobile broadband: EDGE, HSPA & LTE, *White paper for 3G Americas*, September 2006.

[Sch02] H. D. Schotten, J. F. Rößler, System performance gain by interference cancellation in WCDMA dedicated and high-speed downlink channels, *in Proceedings of the 56th Vehicular Technology Conference (VTC) 2002 Fall, Vol. 1, pp. 316-320, Vancouver, Canada*, September 2002.

[Tel99] E. Telatar, Capacity of multi-antenna Gaussian channels, *European Transactions on Telecommunications, Vol. 10, No. 6, pp. 585-595*, 1999.

[Tse05] D. Tse, P. Viswanath, Fundamentals of Wireless Communication, Cambridge University Press, 2005.

[Tuo05] E. Tuomaala, M. Kuusela, Performance of Spatial Multiplexing in High Speed Downlink Packet Access System, *Proceedings of the 5th International Conference on Information, Communications and Signal Processing (ICICS), pp. 936-940, Bangkok, Thailand*, December 2005.

[Uyk05] Z. Uykan, K. Hugl, HSDPA system performance of optical fiber distributed antenna systems in an office environment, *Proceedings of the 16th International Symposium on Personal, Indoor and Mobile Radio Communications (PIMRC), Berlin, Germany*, September 2005.

[Van03] K. Vanganuru, A. Annamalai, Combined Transmit and Receive Antenna Diversity for WCDMA in Multipath Fading Channels, *IEEE Communications Letter, Vol. 7, No. 8, pp. 325-354*, August 2003.

[Ven03] M. Ventola, E. Tuomaala, P. A. Ranta, Performance of dual antenna diversity reception in WCDMA terminals, *Proceedings of the IEEE Vehicular Technology Conference (VTC) 2003 Spring, pp. 1035-1040, Jeju, Korea*, April 2003.

[Wan02] Y.-P. E. Wang, J.-F. T. Cheng, E. Englund, The benefits of advanced receivers for high speed data communications in WCDMA, *Proceedings of the IEEE Vehicular Technology Conference (VTC) 2002 Fall, pp. 132-136, Vancouver, Canada*, September 2002.

APPENDIX 1 STATISTICAL CONFIDENCE ANALYSIS OF THE SIMULATION RESULTS

The used dynamic system simulator has been an important tool for the WCDMA system level studies in recent years. The statistical confidence of the simulation results presented in this thesis are evaluated in this chapter by using a one example test case. Main simulation parameters of the test case are presented in Table 8.

TABLE 8 Simulation parameters for the reliability analysis test case.

Simulation scenario	Macro-cell, 7 Node B's (21 sectors)
Site-to-site distance	2800 m
Cell radius	933 m
Propagation model	Based on [3G01]
Slow fading distribution	log-normal, std 8 dB
Slow fading spatial correlation	50 m
Channel profile	Modified Vehicular A
Path powers	[-3.1, -5.0, -10.4, -13.4, -13.9, -20.4]
UE velocity	3 km/h
MAC-hs packet scheduling	Round Robin
HS-DSCH power	14 W
HS-SCCH power	Power controlled, max 2 W
HARQ processes	6
Max no. of multicodes	10
Outer loop LA BLER target	1 %
CQI granularity	1 dB
CQI error distribution	log-normal, std 1 dB

In this test case a Rake 1×1 receiver is used in a modified ITU Vehicular A channel. The model is modified so that the path delays are integer chip durations. A maximum number of HS-PDSCH codes is 10 and Round Robin scheduler is used. For each simulation a seed is given as a parameter to a random number generator. Based on the seed a random starting position and direction of movement is generated for each UE. Also start times of calls and their duration will change when changing the seed. In addition to this there are several random numbers used in the simulation (e.g. measurement error for CQI) which will change if the seed is changed. All the simulation results depend on different random processes during the simulation run and the results are reproducible with a certain accuracy for a specified level of confidence. An interval estimation can be used to define a confidence interval, which means that the sample, is within a defined interval with a certain probability i.e.

$$P(a \leq \phi \leq b) = 1 - \alpha\,, \tag{55}$$

where the interval $[a, b]$ is a $(1 - \alpha) \cdot 100\%$ confidental interval of ϕ. A probability that the ϕ is not within the interval is α. When the number of samples $n \geq 30$ the standardized normal distribution $N(0, 1)$ can be used to define a confidental interval, which is

$$\left(\overline{x} - z_{\alpha/2} \cdot \frac{s}{\sqrt{n}}, \overline{x} + z_{\alpha/2} \cdot \frac{s}{\sqrt{n}} \right), \tag{56}$$

where $\overline{x}$ is the average value, $\frac{s}{\sqrt{n}}$ is the critical value taken from the standardized normal distribution $N(0, 1)$, s is the standard deviation and n is the number of samples i.e. the number of simulations.

The confidence interval can be used to evaluate the statistical confidence of the simulation results. In the analysis of the simulations ran for this thesis the average cell throughput, HS-DSCH SINR and the user bit rate are taken into account. Average cell throughput is the average instantaneous HS-DSCH throughput in a TTI collected from all the sectors in a simulation area during the whole simulation time. Average HS-DSCH SINR is collected from scheduled mobiles during the whole simulation time. Average user bit rate is calculated by dividing the number of transmitted bits during the call divided by the call time. It is calculated at the end of each call. Due to that there are relatively few samples gathered compared to cell throughput and HS-DSCH SINR, which are gathered every TTI. Thus, also the confidence interval for user bit rate statistic is higher.

Confidence intervals of 90 %, 95 % and 99 % are presented in Table 9 and concerning the cell throughputs they are $\pm$ 0.21 %, $\pm$ 0.32 % and $\pm$ 0.38 % respectively. The confidence intervals were calculated from the simulation results from $n = 35$ simulation runs with different random generator seeds presented in Table 10.

TABLE 9 Statistical confidence intervals.

Variable	90 %	95 %	99 %
Cell throughput	$\pm$ 0.21 %	$\pm$ 0.32 %	$\pm$ 0.38 %
HS-DSCH SINR	$\pm$ 0.10 %	$\pm$ 0.16 %	$\pm$ 0.19 %
User bit rate	$\pm$ 0.68 %	$\pm$ 1.03 %	$\pm$ 1.23 %

TABLE 10 Simulation results from 35 simulation runs with different seeds.

Cell throughput [kbps]	HS-DSCH SINR [dB]	User bit rate [kbps]
1355.25	10.916330	99.0964
1347.99	10.872435	98.7931
1363.74	10.976760	98.2907
1396.10	10.985729	99.0762
1361.52	10.984371	98.3627
1351.00	10.932789	97.6017
1374.49	10.952957	98.7828
1357.10	10.976737	100.4760
1367.57	10.834013	98.3610
1362.63	11.007915	98.7326
1381.83	10.942194	99.8164
1360.12	11.063948	112.4370
1374.23	10.937580	98.8103
1342.82	10.875990	97.1987
1351.62	10.972059	101.3910
1359.41	10.907228	98.2317
1361.17	10.945916	97.4489
1355.37	10.931690	97.7277
1346.49	11.006187	99.0740
1353.88	10.914659	98.0899
1362.34	10.853869	97.9464
1373.12	10.886496	97.6410
1333.41	10.922676	97.3125
1373.72	10.923106	97.8036
1348.20	10.914219	98.6104
1352.43	10.863135	97.4246
1362.85	10.889945	98.4630
1366.84	10.924892	97.9481
1358.64	10.982977	99.0742
1374.44	10.823224	98.0622
1363.16	10.867833	98.2832
1367.25	10.894961	98.1953
1372.08	10.928412	98.5204
1337.31	10.943307	98.4535
1385.11	10.913284	109.5350

APPENDIX 2 SIMULATION TOOL VERIFICATION

The verification and validation of the simulation results provided in this thesis is done by comparing the results to other HSDPA system simulation results provided by various studies. In [Lov03] system level performance of single and dual-antenna rake and LMMSE equalizer receivers were presented. Although the simulation scenario used in that study differs in many ways from the scenario used in the simulations of this thesis, the results are very well aligned, as can be seen in Table 11. The presented results are from proportional fair scheduler simulations.

TABLE 11 Cell throughput gain comparison between this thesis and [Lov03].

Receiver	Gain [%]	[Lov03] Gain [%]
Rake 1×1	0 %	0 %
Rake 1×2	44-57 %	44-50 %
Equ 1×1	25-30 %	24-31 %
Equ 1×2	88-115 %	89-103 %

Also in [Ram03] simulations similar to those presented in this thesis were conducted. Single and dual antenna Rake receiver simulations with and without transmit diversity were conducted in Vehicular A and Pedestrian A channels with round robin and proportional fair schedulers with 3 km/h UE velocity. In Table 12 the comparison of the cell throughputs is presented for a Vehicular A channel.

TABLE 12 Cell throughput and gain comparison between this thesis and [Ram03].

Receiver	RR		PF		[Ram03] RR		PF	
	[kbps]	[%]	[kbps]	[%]	[kbps]	[%]	[kbps]	[%]
Rake 1×1	1049	0 %	1683	0 %	712	0 %	1079	0 %
Rake 2×1, STTD	1019	-3 %	1437	-15 %	695	-2 %	918	-15 %
Rake 2×1, CL1	1528	46 %	2063	23 %	891	25 %	1176	9 %
Rake 1×2	2131	103 %	2706	61 %	1206	69 %	1457	35 %
Rake 2×2, CL1	2378	127 %	2844	69 %	1403	97 %	1552	44 %

As can be seen in Table 12, the results with 1×1 Rake and STTD are nearly

the same. The gain of CL Mode 1 and receive diversity schemes the gains and the absolute throughputs of [Ram03] are lower. The lower throughputs can be explained with the fact that in [Ram03] the amount of power reserved for HSDPA was 9 watts as it was 14 watts in the simulations of this thesis. The difference between the results of this thesis and [Ram03] is clearly proportional to the achieved throughput. As the maximum number of multicodes reserved for HSDPA was 7 in [Ram03] the highest throughputs in that study might be limited by the MCS dynamics. In simulations presented in this thesis a maximum of 10 multicodes were allocated, thus higher throughput with equally good signal quality than in [Ram03] could be achieved.